SUPPORTING APPENDIX

Table S1. RNAi screening results for the three MAPK pathways (ERK, JNK, and p38) in *Drosophila* cells against VSV, SINV, and DCV.

Table S2. dsRNA primers for the RNAi-based screen. The gene symbol, DRSC number, sequence, and references are provided for the indicated dsRNAs.

Figure S1. Summary schematic for the results of the directed RNAi screen for ERK, JNK, and p38 pathways. Genes highlighted in gray represent the *Drosophila* MAPKKK, MAPKK, and MAPK homologues for each pathway, respectively. Genes boxed in red are antiviral for VSV, SINV, and DCV. Genes boxed in black are not antiviral for all three viruses. Genes boxed in blue are transcriptionally induced by VSV infection.

Figure S2. Magnified images from Figure 1B. *Drosophila* cells treated with the indicated dsRNAs challenged with VSV (MOI=0.2), SINV (MOI=5), or DCV (MOI=1.5) and monitored by fluorescence microscopy (virus in green, nuclei in blue). Magnifications of representative images from Figure 1B are provided for (A) VSV (B) SINV and (C) DCV to view individual nuclei (blue) and infected cells (green).

Figure S3. Depletion of ERK pathway components results in increased viral protein expression in *Drosophila* cells. (A-F) Immunoblot analysis of *Drosophila* cells treated with dsRNA targeting the indicated ERK pathway components and infected with (A,B) VSV (MOI=0.2), (C,D) SINV (MOI=5), or (E,F) DCV (MOI=1.5).

Figure S4. Depletion of ERK pathway components results in increased viral RNA levels in *Drosophila* cells. Quantitative RT-PCR analysis of *Drosophila*

cells treated with the indicated dsRNA and infected with the indicated virus (VSV (MOI=0.2), SINV (MOI=5), or DCV (MOI=1.5)). Viral RNA levels are normalized to Rp49 and shown as a relative fold change compared to the control. Mean ± S.D. of three independent experiments is shown; *p<0.05.

Figure S5. Validation of RNAi screen. (A) Quantitative RT-PCR analysis of *Drosophila* cells treated with the indicated dsRNA. Transcript levels are normalized to Rp49 and shown as a relative fold change compared to the control. Mean ± S.D. of three independent experiments is shown; *p<0.05. (B) Immunoblot analysis of *Drosophila* cells treated with two different dsRNAs targeting dErk. (C) *Drosophila* cells treated with the independent dsRNAs challenged with VSV (MOI=0.2) or SINV (MOI=5) and monitored by microscopy (virus in green, nuclei in blue). Quantification of images with mean ± S.D. of three independent experiments; *p < 0.05.

Figure S6. U0126 treatment prevents Erk activation and is antiviral. (A) Immunoblot analysis of *Drosophila* cells treated with insulin (3.4 μM) and/or U0126 (10 μM) for 15 minutes. (B) Representative images of *Drosophila* cells treated with PBS or U0126 (10 μM) and challenged with VSV (MOI=0.2), SINV (MOI=5), or DCV (MOI=1.5) (virus, green; nuclei, blue) as in Figure 1D. (C) Cell number quantification for three independent experiments using automated image analysis of PBS or U0126-treated *Drosophila* cells analyzed with Figure 1D (ns, not significant).

Figure S7. Dose-dependent antiviral effects of U0126. (A) Immunoblot analysis of *Drosophila* cells treated with and the indicated concentration of U0126 in the presence or absence of insulin (3.4 μM). (B) Quantification of the change in percent SINV infection (MOI = 5) over a range of U0126 concentrations performed in duplicate with the mean and range shown.

Figure S8. Full immunoblots shown. Uncropped immunoblots shown from (A) Figure 1E and (B) Figure 1F.

Figure S9. Immunoblot quantification for Figure 1. Quantification of immunoblots of phospho-Erk, total Erk, and tubulin from (A) Figure 1E (B) Figure 1F and (C) Figure 1G. Mean ± S.D. of three independent experiments shown; *p < 0.05.

Figure S10. Magnified images from Figure 2A. *Aedes aegypti* Aag2 cells treated with the indicated dsRNAs were challenged with VSV (MOI=0.01) or SINV (MOI=0.5) and monitored by microscopy (virus, green; nuclei, blue). Representative images are provided for Figure 2A to allow better visualization of individual nuclei (blue) and infected cells (green).

Figure S11. Immunoblot quantification for Figure 2E. Immunoblot quantification for phospho-Erk, total Erk, and tubulin provided for Figure 2E. Mean ± S.D. of three independent experiments; *p < 0.05.

Figure S12. U0126 treatment of Aag2 cells does not alter cell number. Quantification of cell number in Aag cells treated with PBS or U0126 (10 μM) analyzed with Figure 2G for three independent experiments (ns, not significant).

Figure S13. Magnified images from Figure 2F. *Aedes aegypti* Aag2 cells treated with PBS or U0126 (10 μM) and were challenged with VSV (MOI=0.01) or SINV (MOI=0.5) and monitored by microscopy (virus, green; nuclei, blue). Representative images are provided for Figure 2F to allow better visualization of individual nuclei (blue) and infected cells (green).

Figure S14. Immunoblot quantification for Figure 2H. Immunoblot quantification for phospho-Erk, total Erk, and tubulin provided for Figure 2H. Mean ± S.D. of three independent experiments; *p < 0.05.

Figure S15. Immunoblot quantification for Figure 3A. Immunoblot quantification for phospho-Erk and total Erk for Figure 3A. Mean ± S.D. of three independent experiments; *p < 0.05.

Figure S16. Oral treatment with U0126 does not alter feeding behavior or viability of flies. (A) Representative images of flies fed with PBS or U0126 (500 μM) along with red dye for 7 days. (B) A representative survival curve for 50 flies as in (A).

Figure S17. Viral ingestion triggers Erk activation. (A) Immunoblot analysis of wild type flies fed PBS or DCV for 1.5 hours. (B)). Quantification of immunoblots with mean ± S.D. of three independent experiments; *p < 0.05.

Figure S18. Increased infection of the midgut leads to spread outside the epithelium. Flies fed with PBS or U0126 (500 μM) and DCV (25 μL of 1 X 10^12 iu/mL) and virus was removed D3 post infection. Midguts were dissected 7 days post infection and stained for viral antigen and the percentage of intestines with visceral muscle staining were quantified over 5 experiments. (B) Example guts with staining of visceral muscle cells are shown. These are located on the ouside of the gut and have a stereotypic morphology.

Figure S19. Fluorescence images of VSV, SINV, and DCV infection in the insect gut. Female flies orally fed with U0126 (500 μM) and 10 μL of the indicated virus (VSV (1 x 10^8 pfu/mL), SINV (1 X 10^9 pfu/mL), and DCV (1 X 10^12 iu/mL)). Midguts were dissected and stained for viral protein 7 d.p.i. (virus, green; nuclei. blue). Enterocytes are characterized by large nuclei (arrow head) while stem cells have small nuclei (arrow).

Figure S20. Flies with Erk-depleted intestines do not have differences in feeding behavior or viability. (A) Representative images of MyoIA>+ and

MyoIA>Erk IR fed with red dye for 7 days. (B) A representative survival curve for 20 flies as in (A).

Figure S21. Drosophila and Aedes cell lines have similar insulin-sensitivity for ERK activation. Immunoblot analysis of (A) *Drosophila* DL1 or (B) *Aedes Aag2* cells treated with the indicated doses of insulin for 10 minutes.

Figure S22. Insulin treatment of Drosophila cells is protective against viral infection and does not alter cell number. (A) *Drosophila* cells treated with PBS or Insulin (3.4 μM) and challenged with SINV and/or DCV and monitored by microscopy (virus, green; nuclei, blue) from Figure 4A to allow better visualization of individual nuclei (blue) and infected cells (green). (B) Quantification of cell number in *Drosophila* cells treated with PBS or insulin (3.4 μM) from Figure 4A for three independent experiments (ns, not significant).

Figure S23. Insulin treatment of mosquito cells is protective against viral infection and does not alter cell number. (A) *Aedes aegypti Aag2* cells treated with PBS or Insulin (3.4 μM) and challenged with SINV and monitored by microscopy (virus, green; nuclei, blue) from Figure 4C to allow better visualization of individual nuclei (blue) and infected cells (green). (B) Quantification of cell number in insect cells treated with PBS or Insulin (3.4 μM) from Figure 4B for three independent experiments (ns, not significant).

Figure S24. Antiviral activity of insulin is ERK-dependent in *Drosophila* cells. *Drosophila* cells treated with the indicated dsRNAs, treated with either PBS or Insulin (3.4 μM), and challenged with VSV (MOI=0.2). Viral infection was monitored by microscopy 24 hours post infection (virus in green, nuclei in blue). Quantification of percent infected cells with the mean ± S.D. of three independent experiments shown; *$p < 0.05$, ns, not significant.

Figure S25. Immunoblot quantification for Figure 4C. Immunoblot quantification for performed for phospho-Erk and total Erk for Figure 4C with mean ± S.D. of three independent experiments; *p < 0.05.

Figure S26. Oral treatment with insulin does not alter feeding behavior or viability of flies. (A) Representative images of flies fed with PBS control or insulin (83.5 μM) along with red dye for 7 days. (B) A representative survival curve for 50 flies as in (A).

Figure S27. Antiviral activity of insulin is dose-dependent in the *Drosophila* gut. Flies were fed either PBS or Insulin at the indicated doses and orally challenged with DCV (2 μL of 1 X 10^13 iu/mL) for 7 days. DCV infection was analyzed by quantitative RT-PCR, normalized to Rp49 and shown relative to the control. Mean ± S.D. of five independent experiments; *p<0.05.

Figure S28. Antiviral activity of insulin is ERK-dependent in the *Drosophila* gut. Quantitative RT-PCR analysis of MyoIA>+ and MyoIA>Erk IR midguts fed with DCV (2 μL of 1 X 10^13 iu/mL), with and without insulin treatment (83.5 μM), are shown as indicated. Samples were normalized to Rp49, and shown relative to MyoIA>+ DCV-infected flies at 7 days post infection. Mean ± S.D. of three independent experiments (*p<0.05, ns, not significant).

Figure S29. Diptericin B expression is not affected by ERK depletion in enterocytes or viral infection in the *Drosophila* gut. Quantitative RT-PCR analysis of MyoIA>+ and MyoIA>Erk IR midguts for Diptericin B (DiptB) expression, normalized to Rp49 and shown relative to MyoIA>+. Mean ± S.D. of three independent experiments (ns, not significant). (A-C) Quantitative RT-PCR analysis of DiptB in MyoIA>+ flies challenged with the indicated virus, normalized to Rp49, and shown relative to MyoIA>+ uninfected flies at 7 days post infection. Mean ± S.D. of three independent experiments (ns, not significant).

Figure S30. Insulin does not inactivate VSV. VSV treated with PBS or Insulin (3.4 μM) for one hour and subsequently plaqued on BHK cells. Mean ± S.D. of the viral titers for three independent experiments shown (ns, not significant).

Supplementary Methods.

RNAi and Viral Infections in Cell Culture

In brief, cells were passaged into serum free media (SFM) and plated into wells containing dsRNA at 250ng/16,500 cells in 384 well plates. After 1 hour in SFM, complete media was added and cells were incubated at 25°C for three days to allow for gene knockdown. Three days post-dsRNA bathing, cells were infected with the indicated viral inoculum. VSV, SINV, or DCV inocula were added to the existing media in 384 well plates in 10μL of serum-free Schneider's media. VSV and DCV-infected cells were processed at 24 hours post infection. SINV was spinoculated as follows: existing media was removed, virus inoculum was added to wells in 10μL of serum-free Schneider's media, cells were spun at 1200 rpm for 2 hours, then 20μL of 10% serum Schneider's media was added to cells. SINV-infected cells were processed at 36 hours post-infection. Cells were fixed for 10 minutes in 4% formaldehyde, washed in PBS/0.1% TritonX-100 (PBST) twice for 10 minutes each, and blocked in 2% BSA/PBST for 30 minutes. Primary antibody was diluted in block and incubated with cells overnight at 4°C. Cells were washed three times in PBST, and incubated in secondary antibody for one hour at room temperature. Cells were counterstained with Hoescht33342 (Sigma). Following secondary antibody staining and counterstaining, cells were washed an additional three times in PBST and imaged using an automated microscope at 20X (ImageXpress Micro). Images of three sites per wavelength per well were collected and with a minimum of three wells per treatment. Automated image analysis was performed using MetaXpress image analysis software (Cell Scoring) to identify nuclei (Hoescht+) and virus infected (GFP+ or antibody+) cells and thresholding on uninfected wells on each plate. The percent infection was calculated for each site and averaged to obtain a single aggregate value for each well. A student's T-test was performed for significance per

condition for each plate. Lastly, there were three independent biological replicates performed in this manner for each gene. The data is represented as the average fold change and standard deviation from the three independent biological replicates, * $p<0.05$ for three independent experiments. Cells were treated with 3.4 μM bovine insulin and 10 μM U0126 as described (1, 2). For phospho-Erk studies in cells, infections were synchronized by pre-binding virus at 16°C for one hour, then brought to 25°C and processed at the indicated time points.

Fly Infections.

Wild type (w1118) flies were used for drug studies. Myo1A-Gal4 was obtained from E. Baehrecke and UAS-Erk IR (#109108) was obtained from the VDRC. Prior to the day of infection, flies were restricted to a water-only diet for 12 hours and starved for 30 minutes prior to feeding to synchronize ingestion. The food contained 5% sucrose plus dye in addition to the indicated treatment. 83.5 μM bovine insulin was used as described (3) unless otherwise indicated and mixing experiments demonstrated no change in infectivity of VSV when mixed with insulin (Figure S30). 500 μM U0126 was used as described (1, 4). Flies were fed 10 μL of the following concentrations of virus: VSV (1 x 10^8 pfu/mL), SINV (1 X 10^9 pfu/mL), and DCV (1 X 10^12 iu/mL), unless otherwise indicated. For the U0126 experiments, food and virus was changed every 3 days. For the insulin experiments, insulin was only provided for the first 3 days, subsequently food and virus was changed every 3 days. For immunoblots, 15 fly guts were dissected in PBS and processed in RIPA buffer, protease inhibitor cocktail (PP2, PP3) and PMSF as described (5). For RNA, 15 fly guts were dissected in PBS and then processed using Trizol as per the manufacturer's protocol and previously described (6). For microscopy, fly guts were dissected as described (6). In brief, 5-10 guts per experiment, for at least three independent experiments were dissected in PBS, fixed in 4% formaldehyde solution for 30 minutes, rinsed three times in PBS, and blocked with 5% normal donkey serum for 45 minutes at room temperature. Primary antibodies were incubated overnight at 4ºC (DCV capsid 1:5000), secondary antibodies with Hoescht 33342 were used at 1:1000 and

incubated for 1 hour at room temperature. Samples were subsequently washed three times. Coverslips were mounted using Vectashield and imaged using 20X and 40X objectives with a Leica DMI 4000 B fluorescent microscope.

Plaque assays.

Virus was tittered on BHK cells, as detailed in (7).

Quantification of blots.

Immunoblots were quantified using ImageJ software and the data is displayed as the mean ± SD for three independent experiments. The student's T-test was used to determine significance.

Supplementary References

1. Zhang W, Thompson BJ, Hietakangas V, & Cohen SM (2011) MAPK/ERK signaling regulates insulin sensitivity to control glucose metabolism in Drosophila. (Translated from eng) *PLoS Genet* 7(12):e1002429 (in eng).
2. Friedman A & Perrimon N (2006) A functional RNAi screen for regulators of receptor tyrosine kinase and ERK signalling. (Translated from eng) *Nature* 444(7116):230-234 (in eng).
3. Kang MA, Mott TM, Tapley EC, Lewis EE, & Luckhart S (2008) Insulin regulates aging and oxidative stress in Anopheles stephensi. (Translated from eng) *J Exp Biol* 211(Pt 5):741-748 (in eng).
4. Bangi E, Garza D, & Hild M (2011) In vivo analysis of compound activity and mechanism of action using epistasis in Drosophila. (Translated from eng) *J Chem Biol* 4(2):55-68 (in eng).
5. Xu J*, et al.* (2012) Transcriptional pausing controls a rapid antiviral innate immune response in Drosophila. (Translated from eng) *Cell Host Microbe* 12(4):531-543 (in eng).
6. Ohlstein B & Spradling A (2006) The adult Drosophila posterior midgut is maintained by pluripotent stem cells. (Translated from eng) *Nature* 439(7075):470-474 (in eng).
7. Shelly S, Lukinova N, Bambina S, Berman A, & Cherry S (2009) Autophagy is an essential component of Drosophila immunity against vesicular stomatitis virus. (Translated from eng) *Immunity* 30(4):588-598 (in eng).

Table S1: RNAi Screening of MAPK components – VSV, SINV, DCV

Gene Name	Human Homologue	MAPK Pathway	VSV (Fold Change)	SINV (Fold Change)	DCV (Fold Change)
Bgal (Control)	-	-	1.0	1.0	1.0
GFP (Control)	-	-	0.1*	0.2*	-
DCV Pro (Control)	-	-	-	-	0.03*
dSos	SOS1	Erk	2.3*	3.0*	1.6*
dRas	KRAS	Erk	2.0*	2.3*	1.8*
dMek	MAPK2K1	Erk	2.1*	5.4*	2.2*
dErk	MAPK1	Erk	1.9*	1.9*	2.0*
cnk	CNKSR2	Erk	2.5*	1.8*	1.8*
ksr	KSR1/2	Erk	2.8*	3.6*	1.2*
hep	MAP2K7	JNK	0.8	1.0	1.1
bsk	MAPK10	JNK	1.0	1.0	1.4
lic	MAP2K3	p38	1.4	0.7	1.3
p38a	MAPK14	p38	1.4	2.2	1.4
p38b	MAPK14	p38	1.1	2.0	1.2

* $p < 0.05$ in 3 independent experiments

Table S2. dsRNA primers for the RNAi-based screen

Gene Symbol	DRSC Number	Primer Name	Sequence	References
dSos	DRSC30697	dSos T7 F	TAATACGACTCACTATAGGAACGAGCAG GAGAAAAGCAA	Zhou et al., Mol Cell. 2008 Nov 21;32(4):592-9. Comparative analysis of argonaute-dependent small RNA pathways in Drosophila.
		dSos T7 R	TAATACGACTCACTATAGGGTTGCATAAT AGCCAGGCGT	
dSos 2	DRSC03439	dSos' T7 F	TAATACGACTCACTATAGGGGCCAAGGA GGTGATCAAC	Friedman, et al. Nature. 2006 Nov 9;444(7116): 230-4. A functional RNAi screen for regulators of receptor tyrosine kinase and ERK signalling.
		dSos' T7 R	TAATACGACTCACTATAGGTCACCTCGT AAATGTCCATTAT	
dRas	DRSC16814	dRas T7 F	TAATACGACTCACTATAGGTCTTGCCTG CTCGTTGTT	Friedman, et al. Nature. 2006 Nov 9;444(7116): 230-4. A functional RNAi screen for regulators of receptor tyrosine kinase and ERK signalling.
		dRas T7 R	TAATACGACTCACTATAGGACCTGCCTG CTGGACATC	
dMek	DRSC18462	dMek T7 F	TAATACGACTCACTATAGGACGAGGATC TGGAGAAGCTG	Zhou et al., Mol Cell. 2008 Nov 21;32(4):592-9. Comparative analysis of argonaute-dependent small RNA pathways in Drosophila.
		dMek T7 R	TAATACGACTCACTATAGGCTACGGGTG CCCACAAAG	
dMek 2	DRSC27547	dMek' T7 F	TAATACGACTCACTATAGGGCAGATCTC AAGACCCTGCT	
		dMek' T7 R	TAATACGACTCACTATAGGCGTCTAGTT GGGCGACGTAT	
dErk	DRSC21814	dErk T7 F	TAATACGACTCACTATAGGAGTTTGTCT CATTTCAGTATGTT	Friedman, et al. Nature. 2006 Nov 9;444(7116): 230-4. A functional RNAi screen for regulators of receptor tyrosine kinase and ERK signalling.
		dErk T7 R	TAATACGACTCACTATAGGCTTGCATAC CTTCCATTCCC	
dErk 2	DRSC20742	dErk' T7 F	TAATACGACTCACTATAGGCTTTGGATT GGCTCGTATTG	Bakal et al., Science. 2008 Oct 17;322(5900): 453-6. Phosphorylation networks regulating JNK activity in diverse genetic backgrounds.
		dErk' T7 R	TAATACGACTCACTATAGGAGGATCATA ATATTGCTCTAAATAG	
cnk	DRSC07595	cnk T7 F	TAATACGACTCACTATAGGGACCCTTAA AAAGAAGCACAG	Friedman, et al. Nature. 2006 Nov 9;444(7116): 230-4. A functional RNAi screen for regulators of receptor tyrosine kinase and ERK signalling.
		cnk T7 R	TAATACGACTCACTATAGGCATTGACTC CTTGTTGCCTT	

ksr	DRSC12379	ksr T7 F	TAATACGACTCACTATAGGCACCGACTGCAAGTACATC	Friedman, et al. Nature. 2006 Nov 9;444(7116): 230-4. A functional RNAi screen for regulators of receptor tyrosine kinase and ERK signalling.
		ksr T7 R	TAATACGACTCACTATAGGCTCATGTGCCCGTTGGAG	
hep	DRSC20337	hep T7 F	TAATACGACTCACTATAGGGTGGTCCCGGTGGTGGA	
		hep T7 R	TAATACGACTCACTATAGGACCTTGCCCAGGATCTGTT	
bsk	DRSC36595	bsk T7 F	TAATACGACTCACTATAGGTTTAGAGTGCAGTCGGCCTT	Bakal et al., Science. 2008 Oct 17;322(5900): 453-6. Phosphorylation networks regulating JNK activity in diverse genetic backgrounds.
		bsk T7 R	TAATACGACTCACTATAGGAAATGTAACCCATGCCAAGC	
bsk 2	DRSC40727	bsk' T7 F	TAATACGACTCACTATAGGTCTGTCGTGATCCAAGTCCA	
		bsk' T7 R	TAATACGACTCACTATAGGTATCACCCAGCAAAATGTGG	
Lic	DRSC20347	Lic T7 F	TAATACGACTCACTATAGGCCCGCCACGCAACCT	Akimana et al., PLoS One. 2010 Jun 11;5(6):e11025. Host factors required for modulation of phagosome biogenesis and proliferation of Francisella tularensis within the cytosol.
		Lic T7 R	TAATACGACTCACTATAGGCCCAGCACGCTTTCCTC	
p38a	DRSC16743	p38a T7 F	TAATACGACTCACTATAGGTACCAGACGAACCCTCTTC	Vig et al., Science. 2006 May 26;312(5777): 1220-3. CRACM1 is a plasma membrane protein essential for store-operated Ca2+ entry.
		p38a T7 R	TAATACGACTCACTATAGGACTGGATGTAGGAACGTGC	
p38b	DRSC36754	p38b T7 F	TAATACGACTCACTATAGGAAGCACATGGATCACGAGAA	
		p38b T7 R	TAATACGACTCACTATAGGTATCCGGTCATCTCGCTTTC	

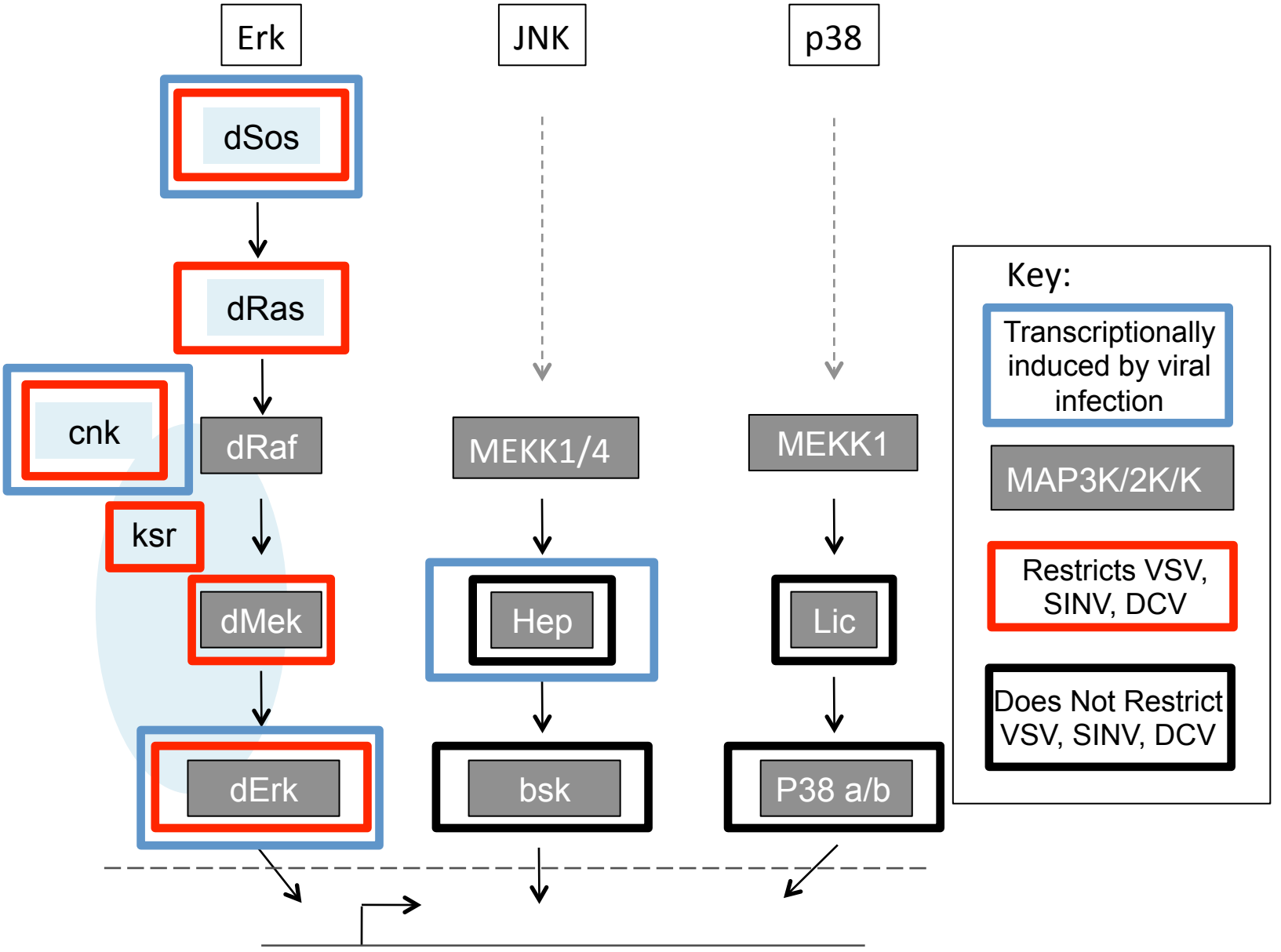
Erk
JNK
p38
dSos
dRas
cnk
dRaf
ksr
dMek
dErk
MEKK1/4
Hep
bsk
MEKK1
Lic
P38 a/b
Key:
Transcriptionally induced by viral infection
MAP3K/2K/K
Restricts VSV, SINV, DCV
Does Not Restrict VSV, SINV, DCV

Figure S1

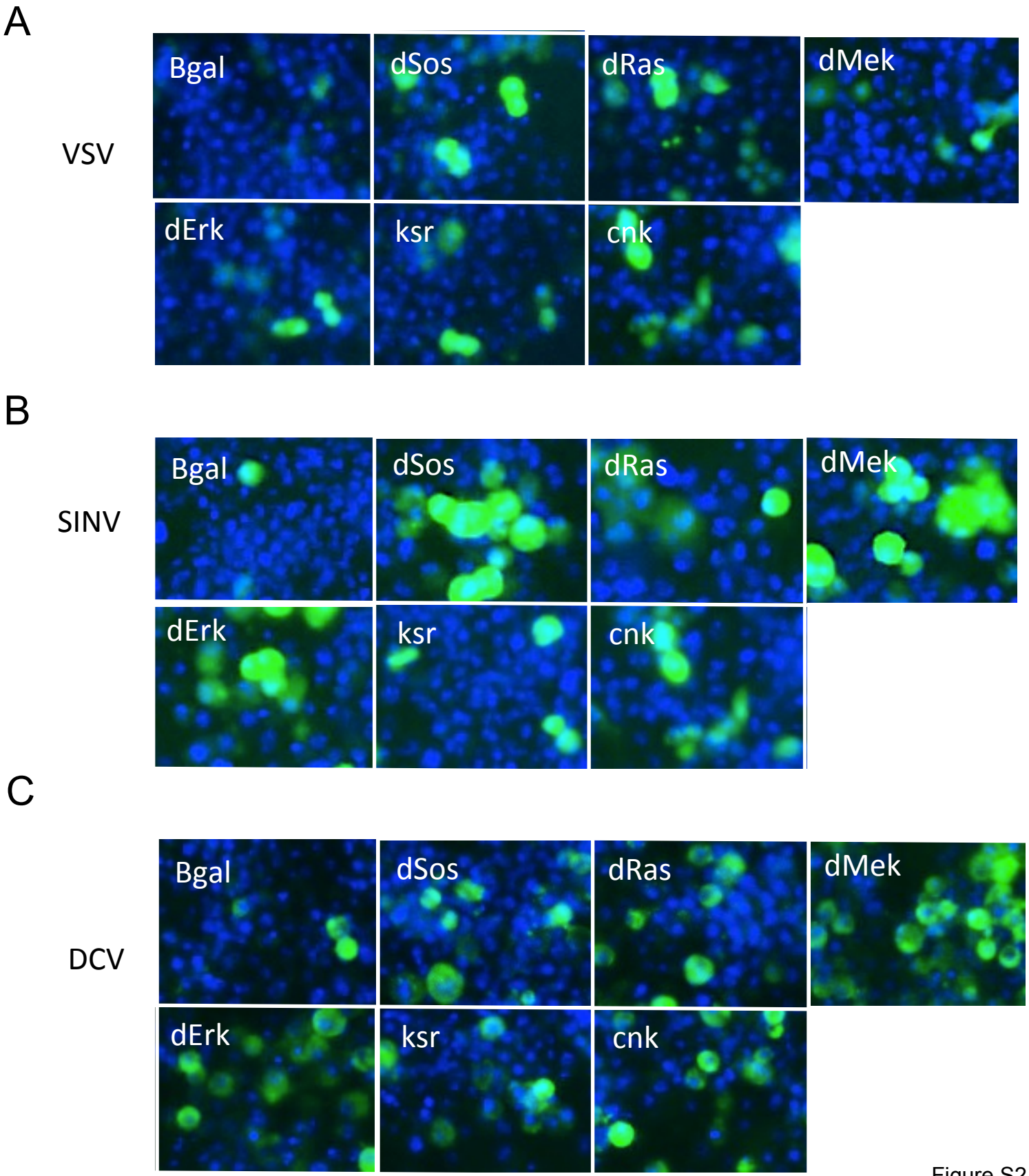
A
VSV
Bgal
dSos
dRas
dMek
dErk
ksr
cnk
B
SINV
Bgal
dSos
dRas
dMek
dErk
ksr
cnk
C
DCV
Bgal
dSos
dRas
dMek
dErk
ksr
cnk

Figure S2

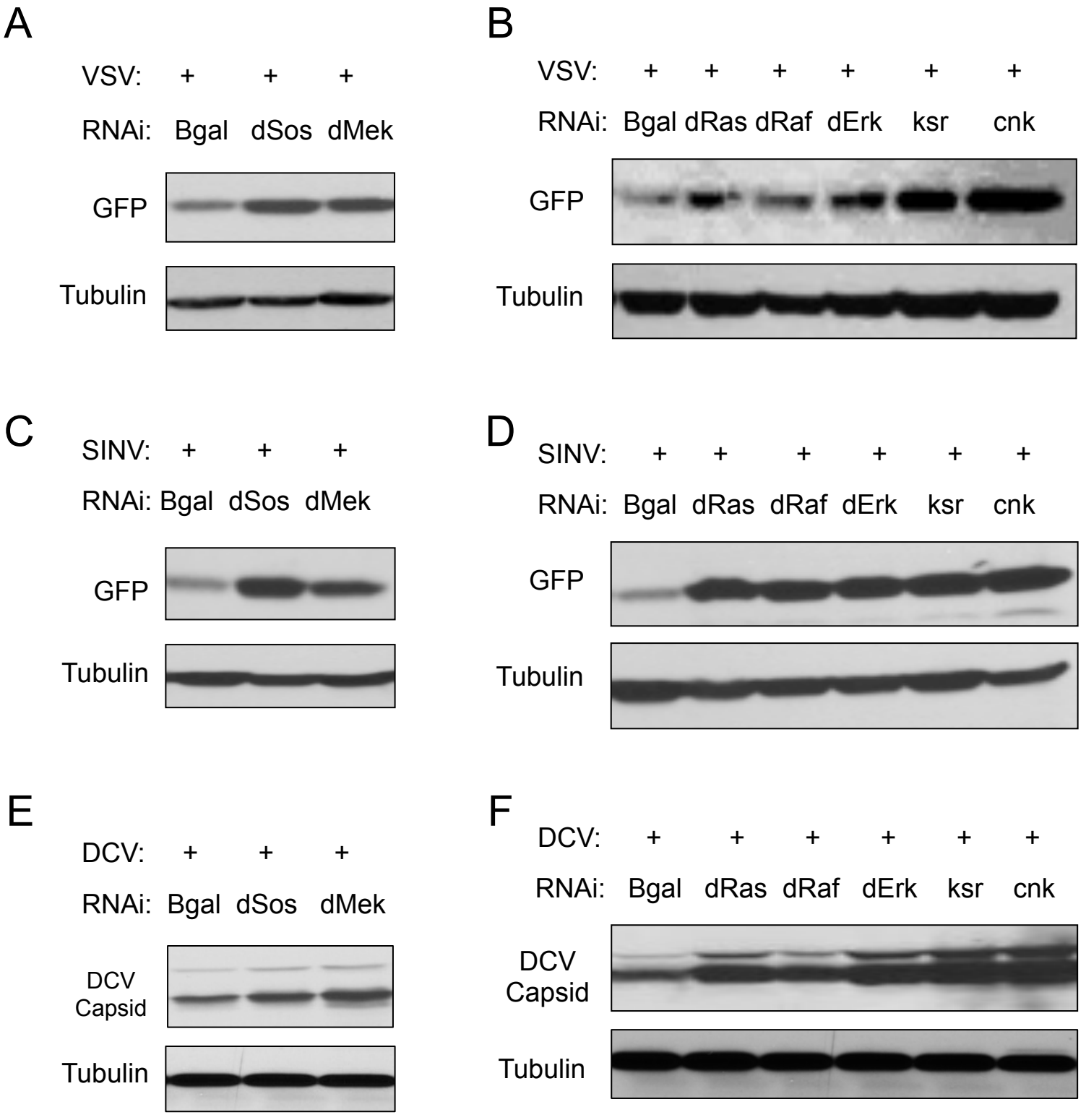
A
VSV: + + +
RNAi: Bgal dSos dMek
GFP
Tubulin
B
VSV: + + + + + +
RNAi: Bgal dRas dRaf dErk ksr cnk
GFP
Tubulin
C
SINV: + + +
RNAi: Bgal dSos dMek
GFP
Tubulin
D
SINV: + + + + + +
RNAi: Bgal dRas dRaf dErk ksr cnk
GFP
Tubulin
E
DCV: + + +
RNAi: Bgal dSos dMek
DCV Capsid
Tubulin
F
DCV: + + + + + +
RNAi: Bgal dRas dRaf dErk ksr cnk
DCV Capsid
Tubulin

Figure S3

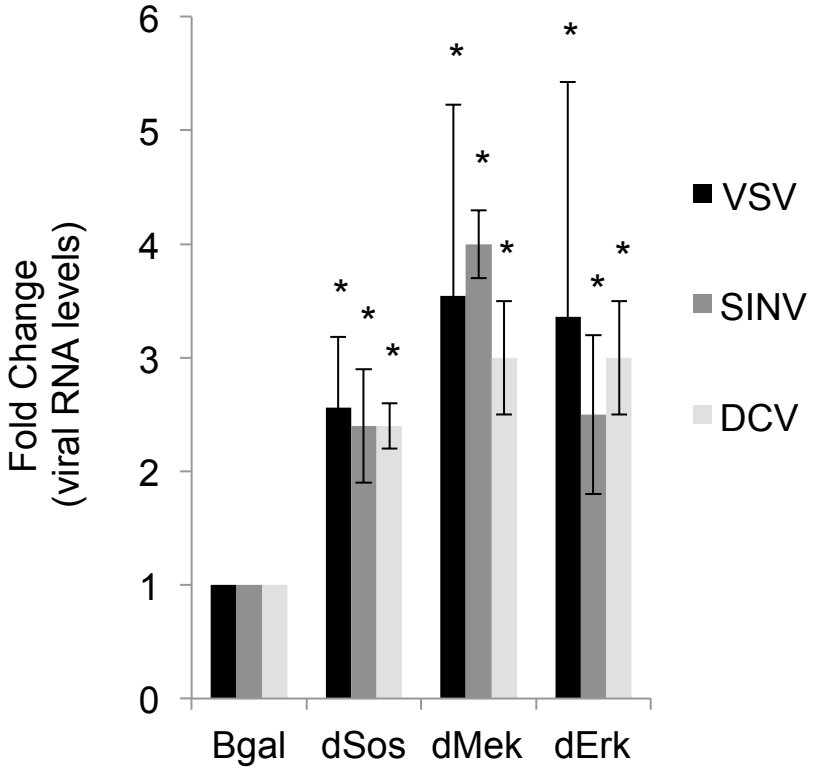
Fold Change
(viral RNA levels)
6
5
4
3
2
1
0
Bgal
dSos
dMek
dErk
VSV
SINV
DCV
*

Figure S4

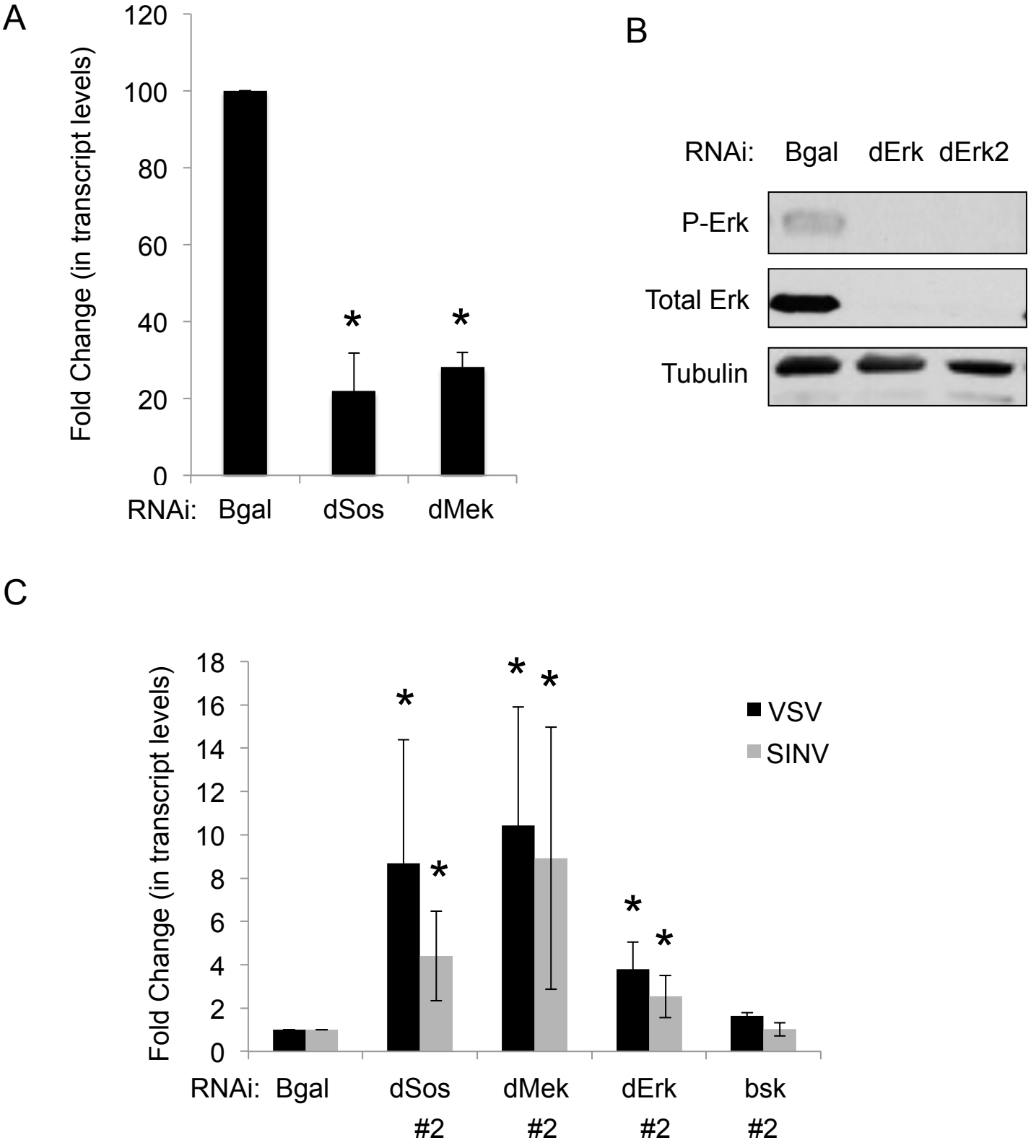
A
120
100
80
60
40
20
0
Fold Change (in transcript levels)
*
*
RNAi: Bgal dSos dMek
B
RNAi: Bgal dErk dErk2
P-Erk
Total Erk
Tubulin
C
18
16
14
12
10
8
6
4
2
0
Fold Change (in transcript levels)
VSV
SINV
RNAi: Bgal dSos #2 dMek #2 dErk #2 bsk #2

Figure S5

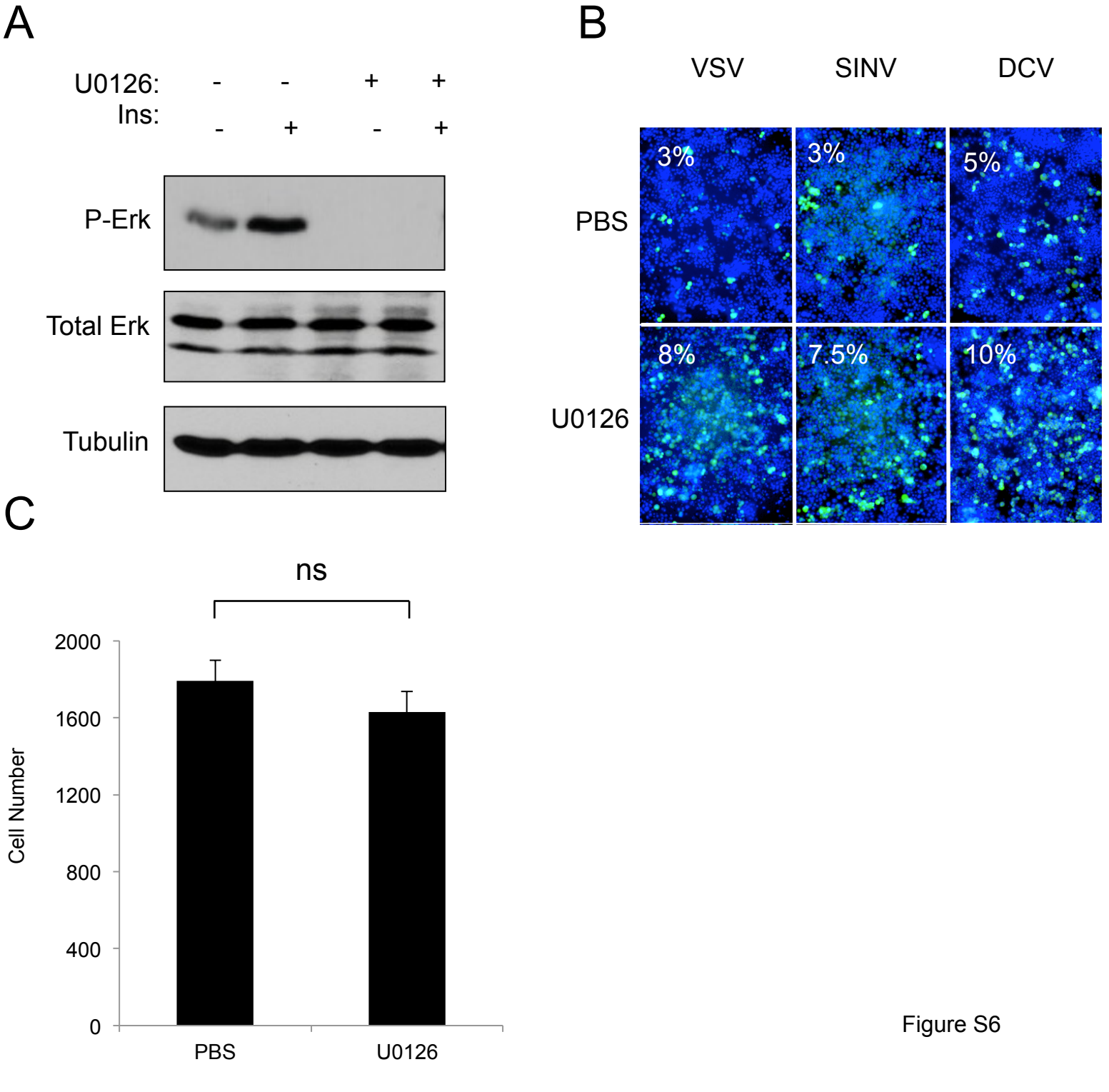
A
U0126: - - + +
Ins: - + - +
P-Erk
Total Erk
Tubulin
B
VSV
SINV
DCV
PBS
U0126
3%
3%
5%
8%
7.5%
10%
C
ns
2000
1600
1200
800
400
0
Cell Number
PBS
U0126

Figure S6

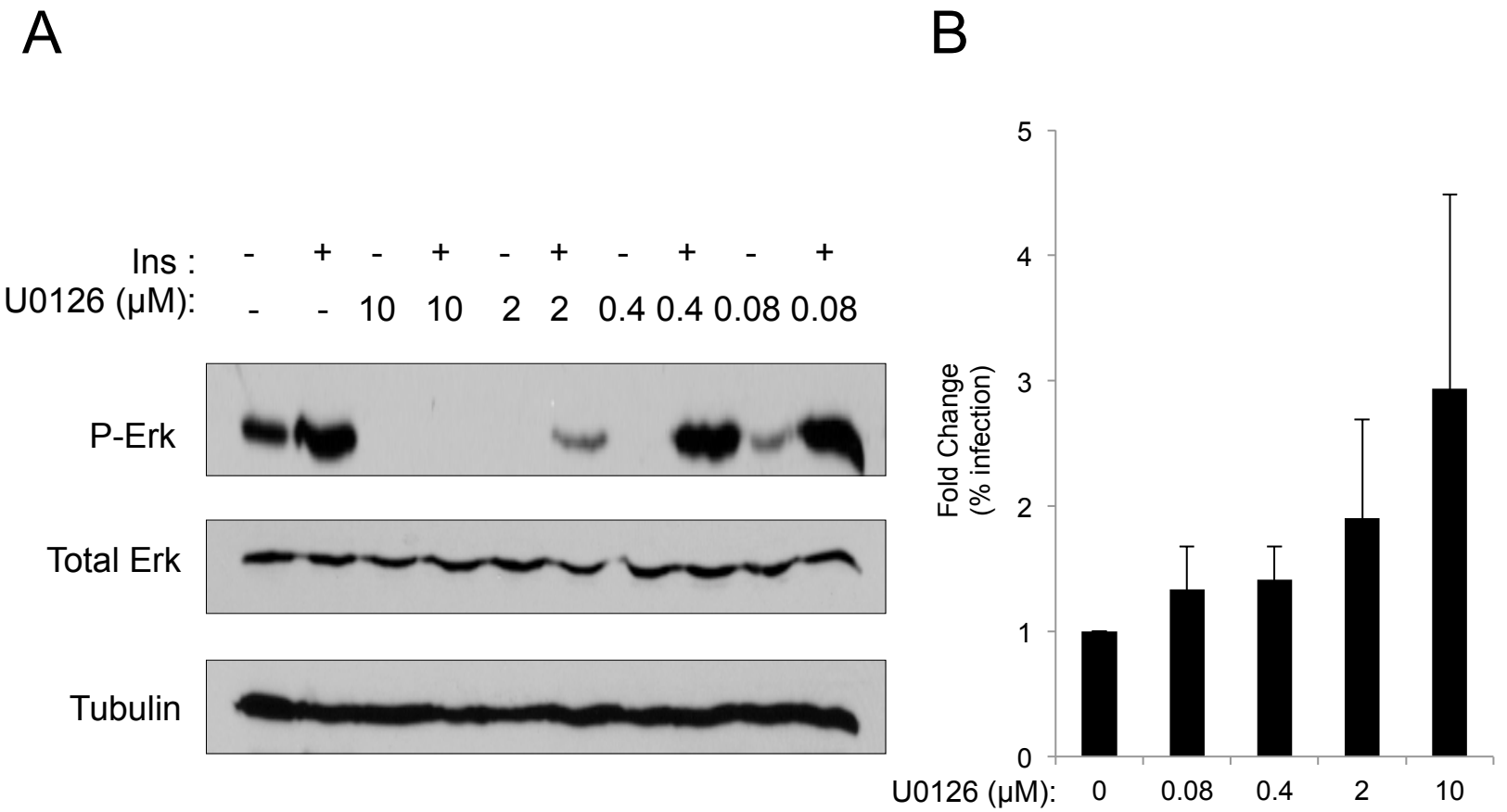
A
Ins : - + - + - + - + - +
U0126 (μM): - - 10 10 2 2 0.4 0.4 0.08 0.08
P-Erk
Total Erk
Tubulin
B
Fold Change (% infection)
0
1
2
3
4
5
U0126 (μM): 0 0.08 0.4 2 10

Figure S7

Figure S8

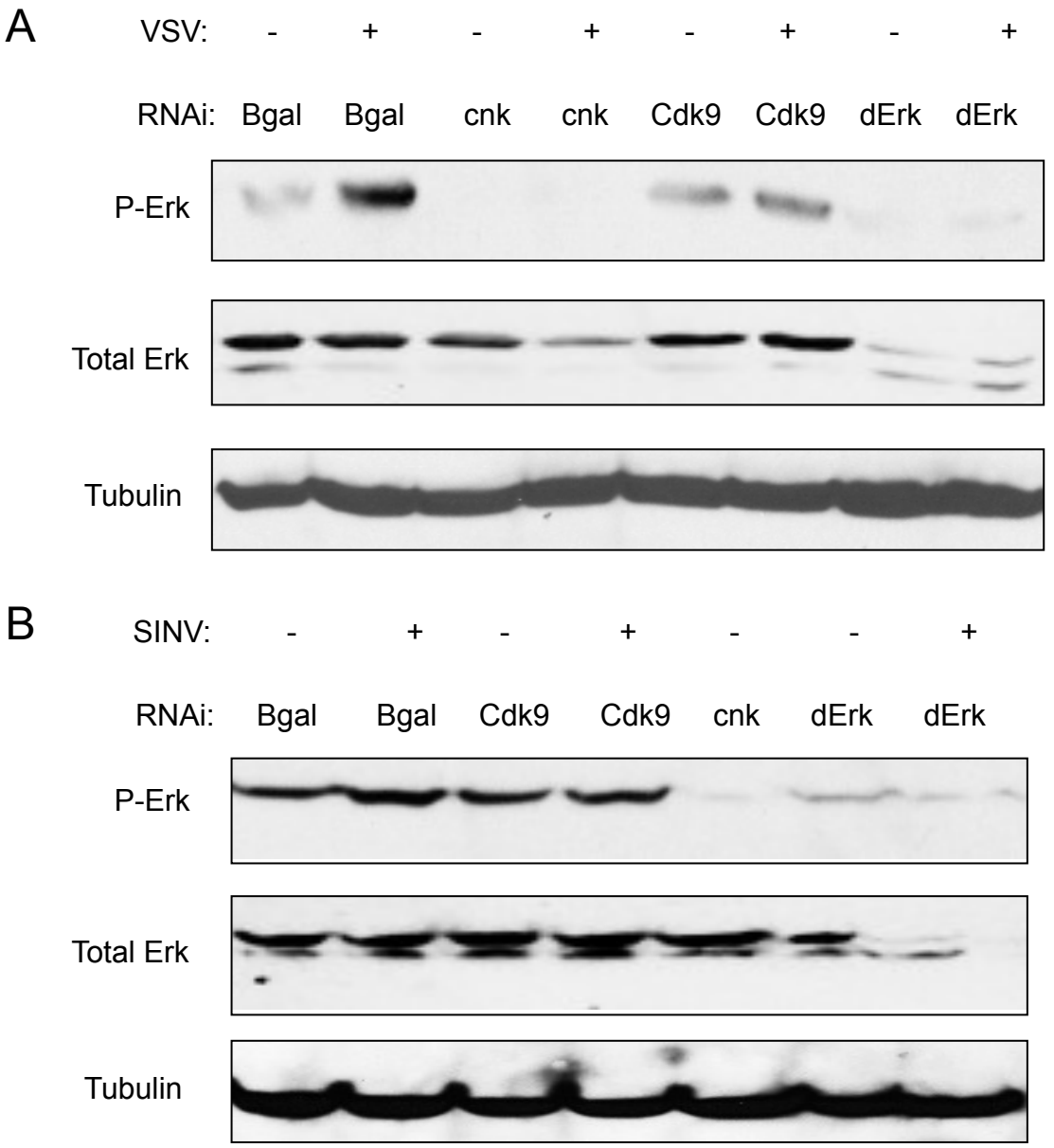
A
VSV: - + - + - + - +
RNAi: Bgal Bgal cnk cnk Cdk9 Cdk9 dErk dErk
P-Erk
Total Erk
Tubulin
B
SINV: - + - + - - +
RNAi: Bgal Bgal Cdk9 Cdk9 cnk dErk dErk
P-Erk
Total Erk
Tubulin

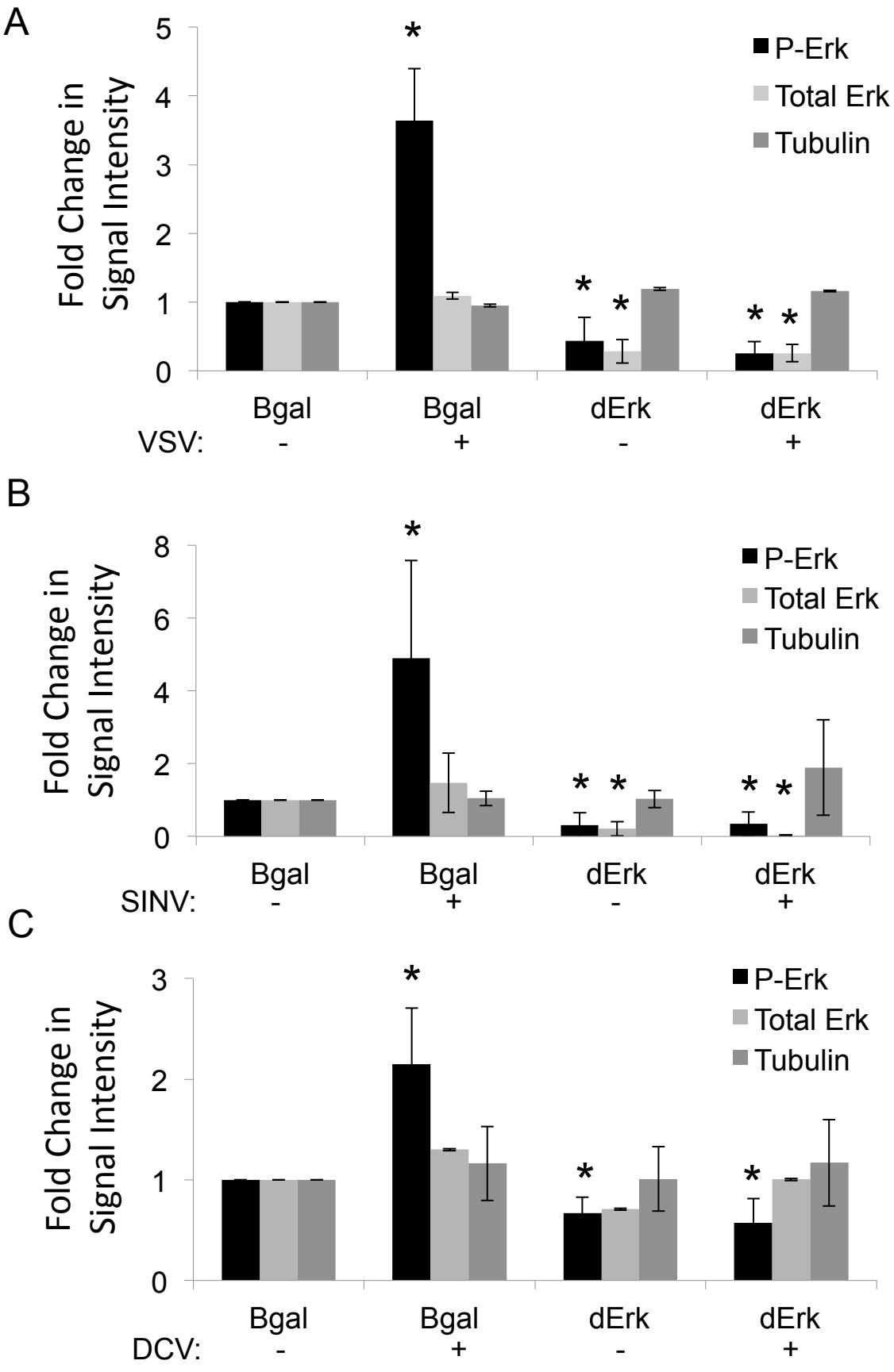
A
Fold Change in Signal Intensity
5
4
3
2
1
0
P-Erk
Total Erk
Tubulin
Bgal
Bgal
dErk
dErk
VSV:
-
+
-
+
B
Fold Change in Signal Intensity
8
6
4
2
0
P-Erk
Total Erk
Tubulin
Bgal
Bgal
dErk
dErk
SINV:
-
+
-
+
C
Fold Change in Signal Intensity
3
2
1
0
P-Erk
Total Erk
Tubulin
Bgal
Bgal
dErk
dErk
DCV:
-
+
-
+

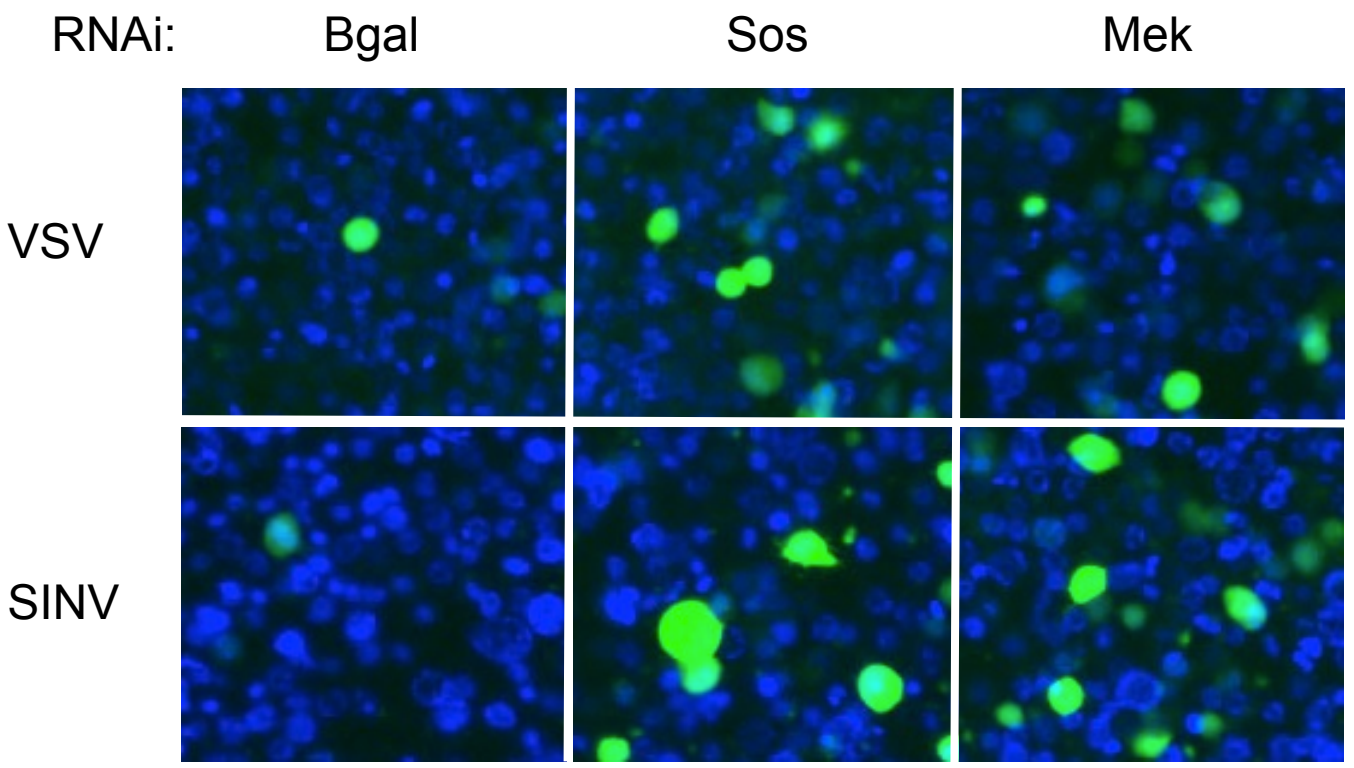
RNAi:
Bgal
Sos
Mek
VSV
SINV

Figure S11

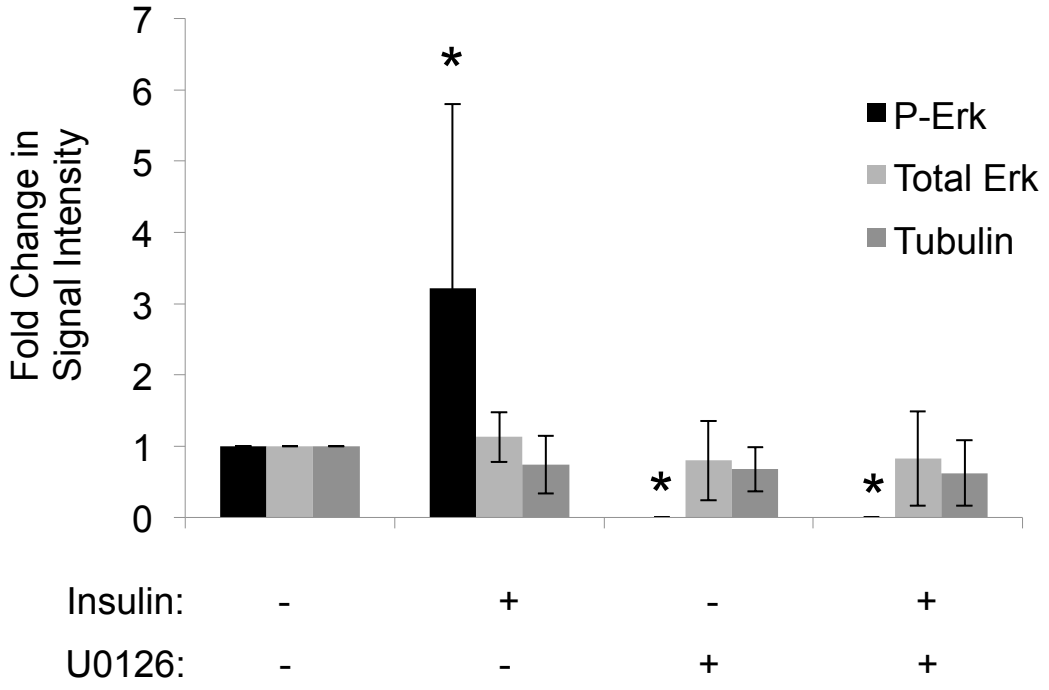
Fold Change in Signal Intensity
7
6
5
4
3
2
1
0
*
*
*
P-Erk
Total Erk
Tubulin
Insulin: - + - +
U0126: - - + +

Figure S12

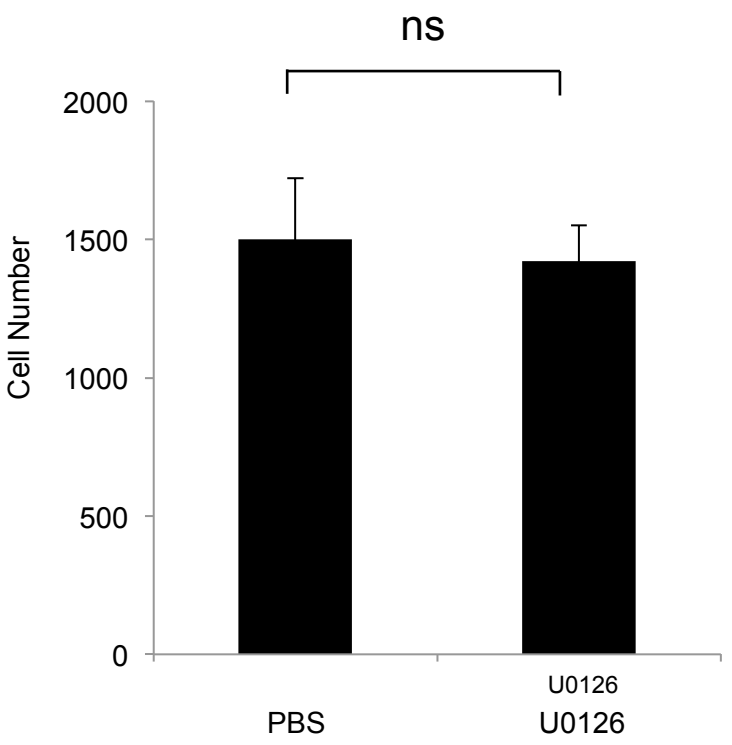

Figure S13

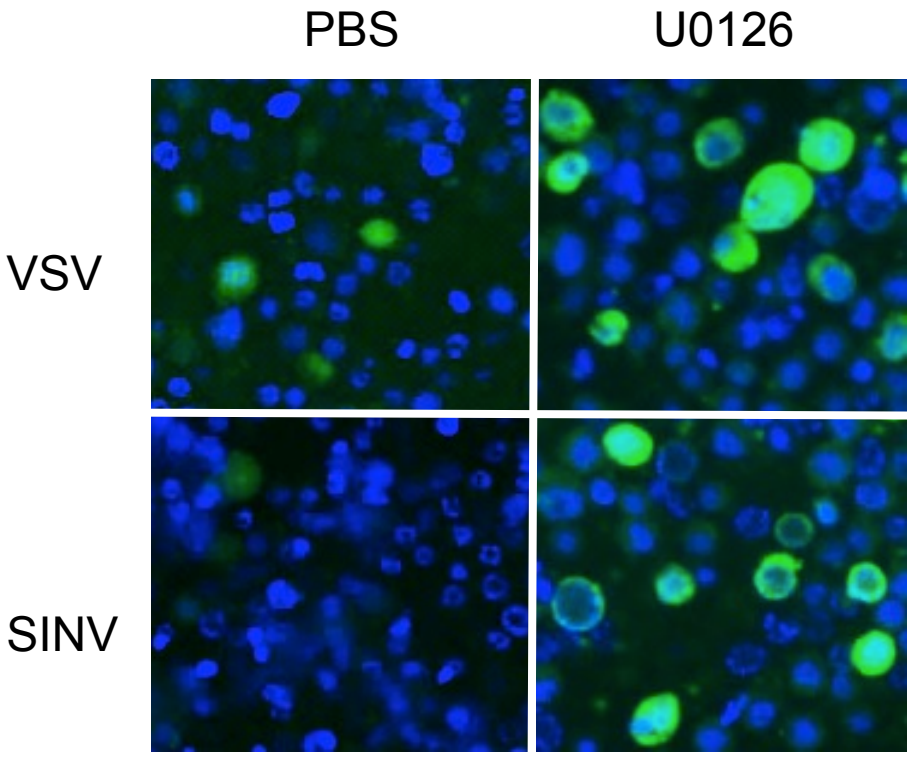

Figure S14

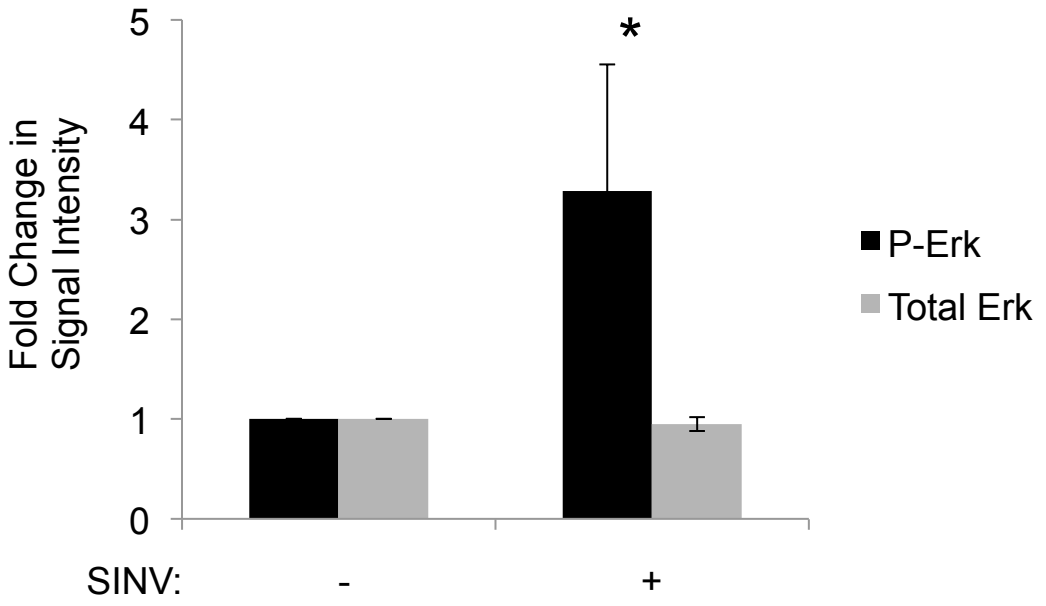

Figure S15

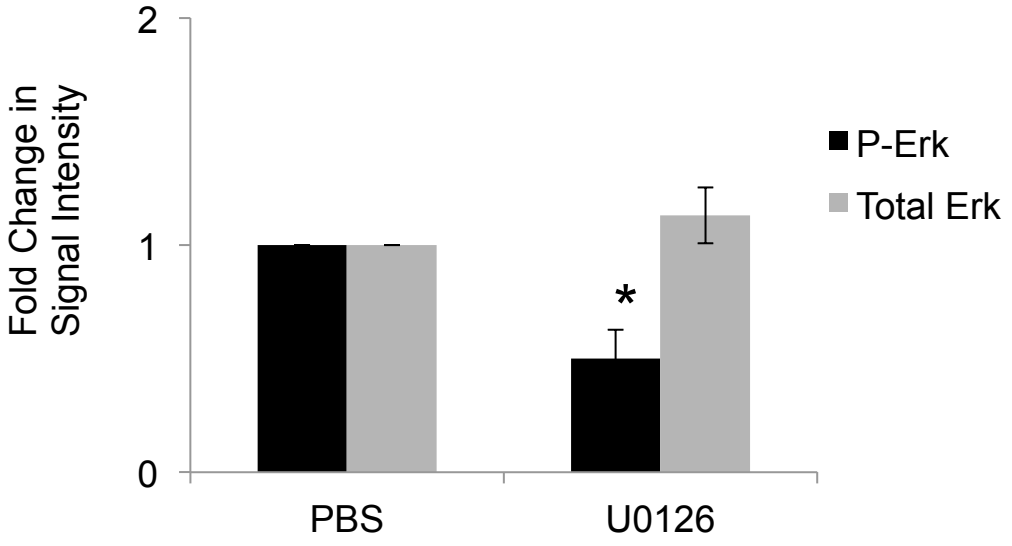
Fold Change in Signal Intensity
2
1
0
*
P-Erk
Total Erk
PBS
U0126

A


PBS
U0126

B

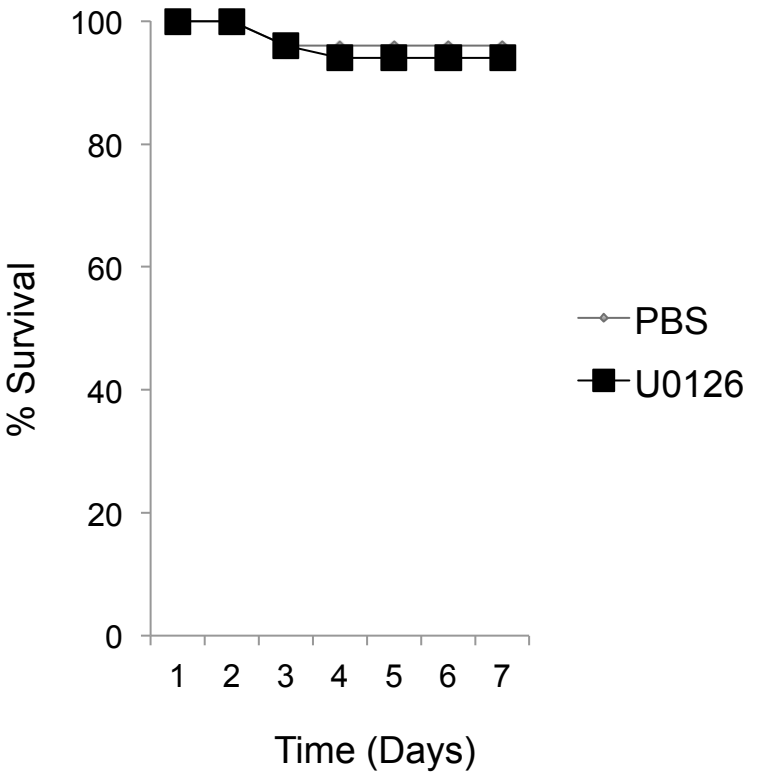
100
80
60
40
20
0
% Survival
1
2
3
4
5
6
7
Time (Days)
PBS
U0126

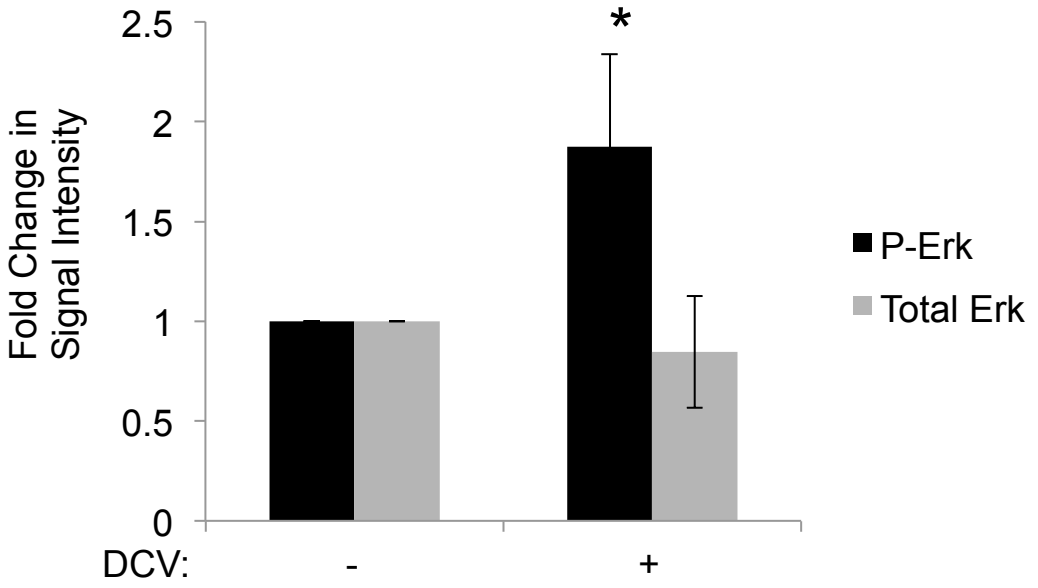
2.5
2
1.5
1
0.5
0
Fold Change in Signal Intensity
*
P-Erk
Total Erk
DCV:
-
+

Figure S17

A

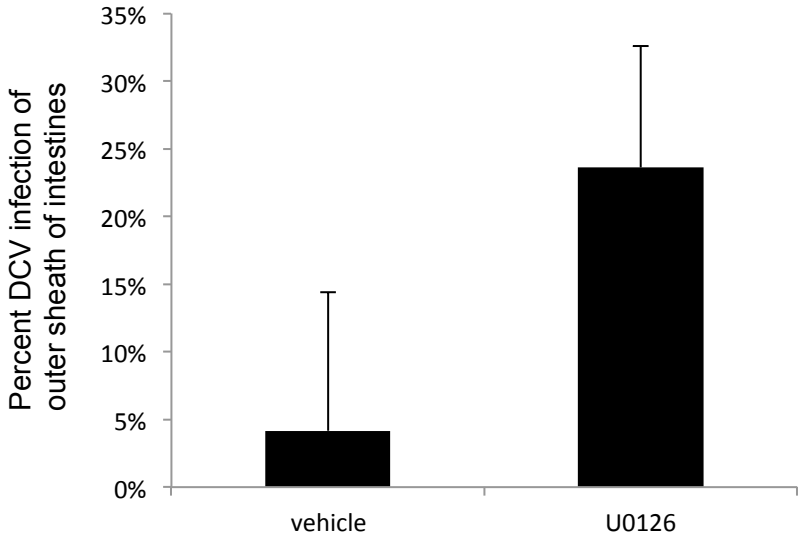

B

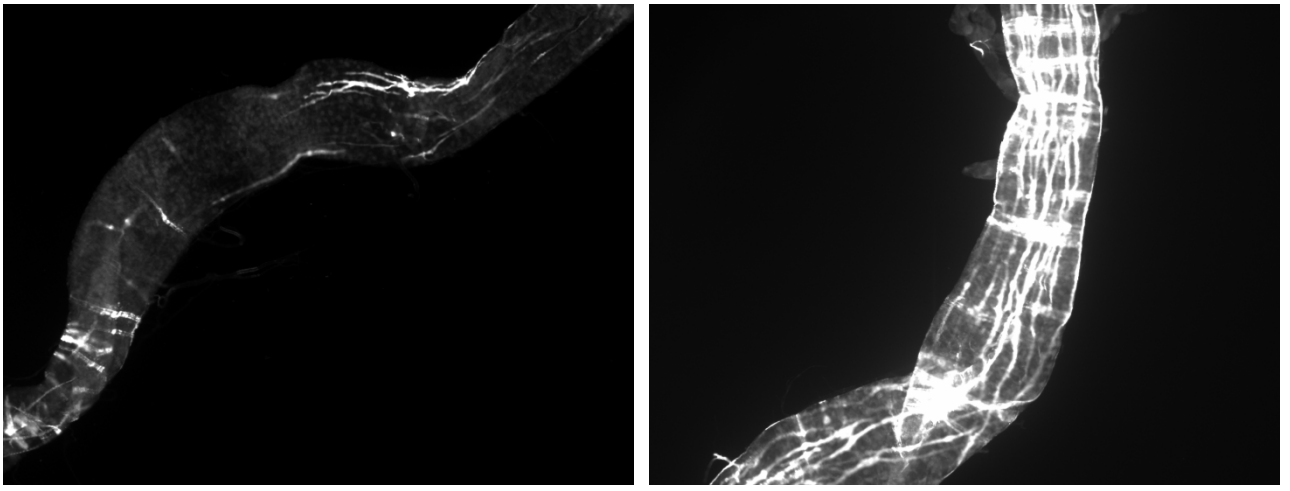

Figure S18

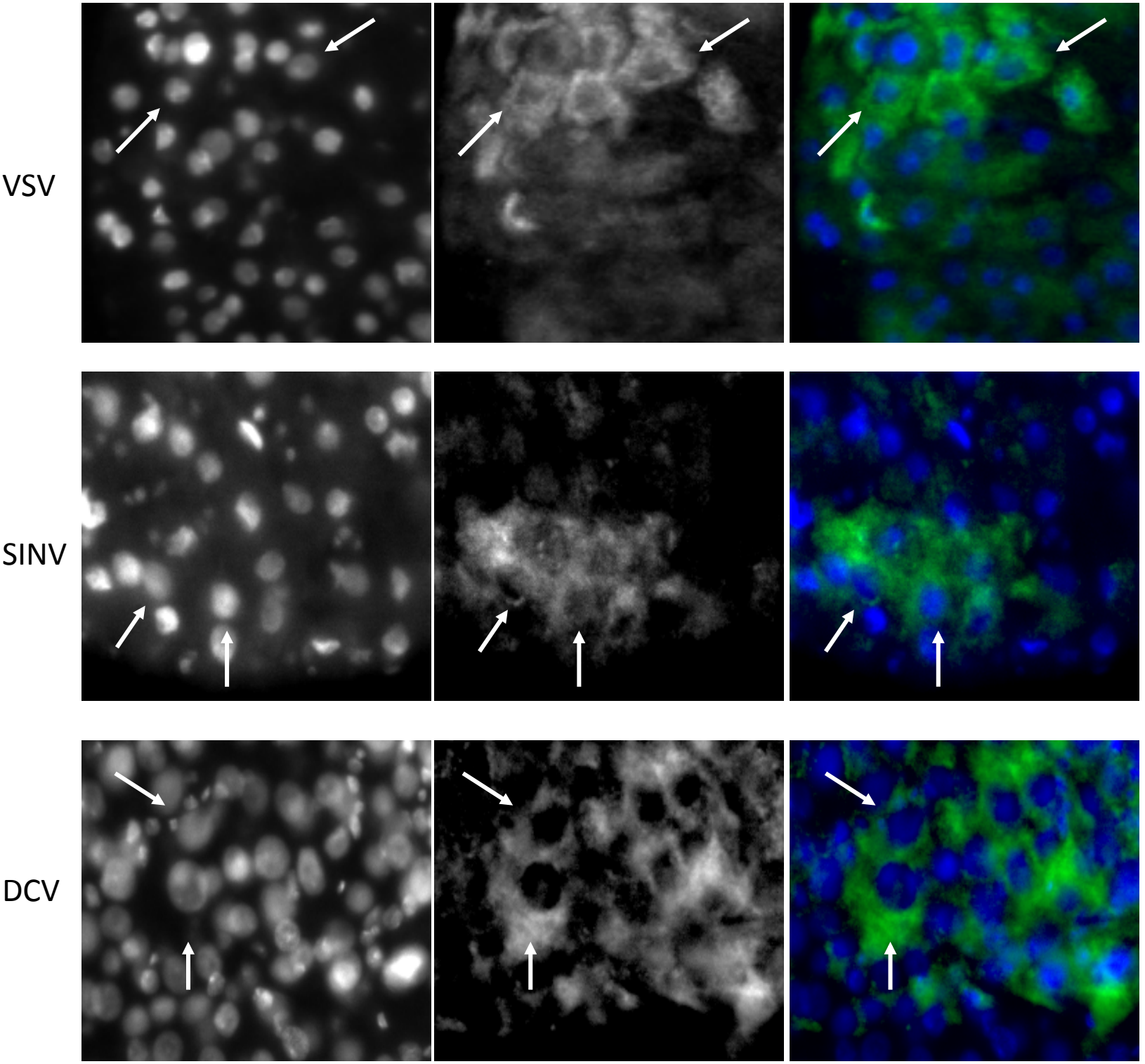
VSV
SINV
DCV

A


MyoIA>+
MyoIA>Erk IR

B

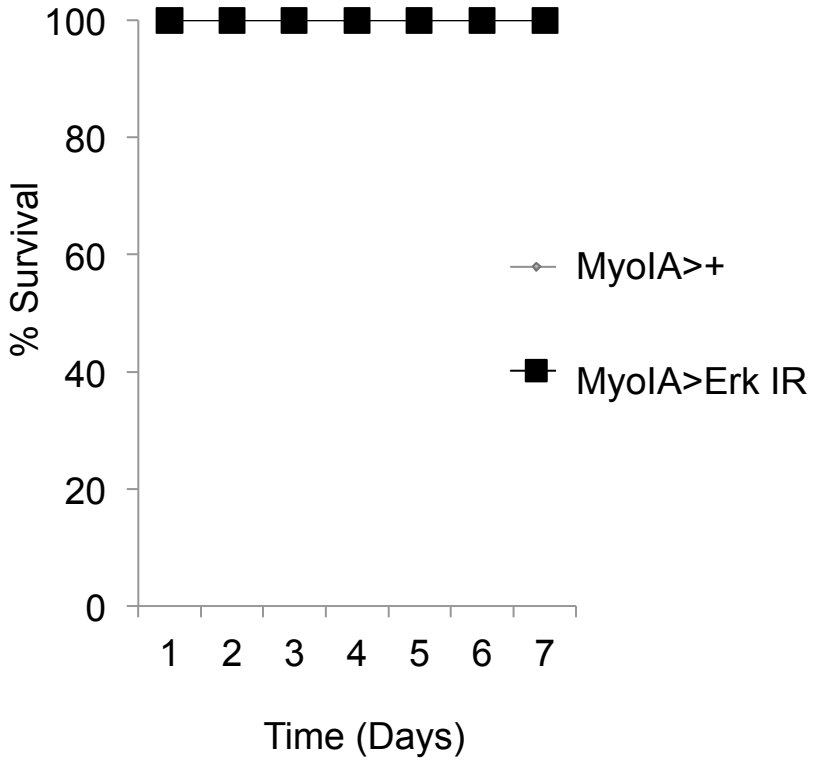
100
80
60
40
20
0
% Survival
1
2
3
4
5
6
7
Time (Days)
MyoIA>+
MyoIA>Erk IR

A

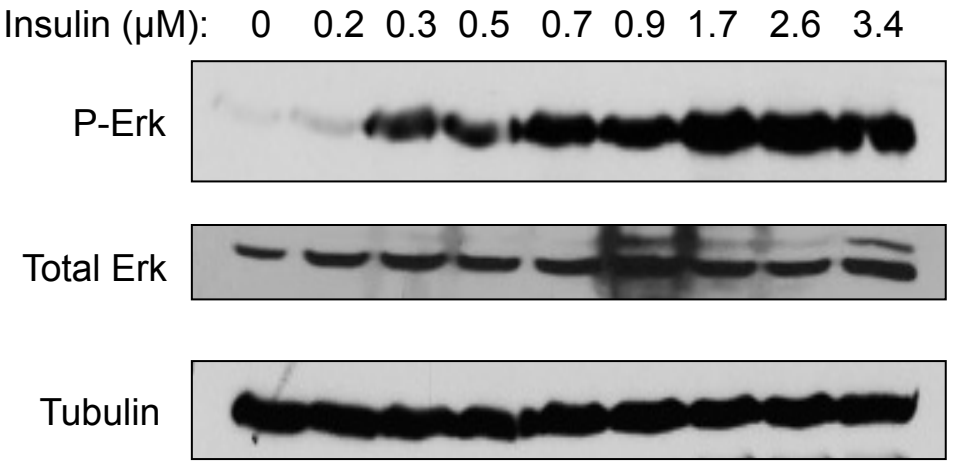

B

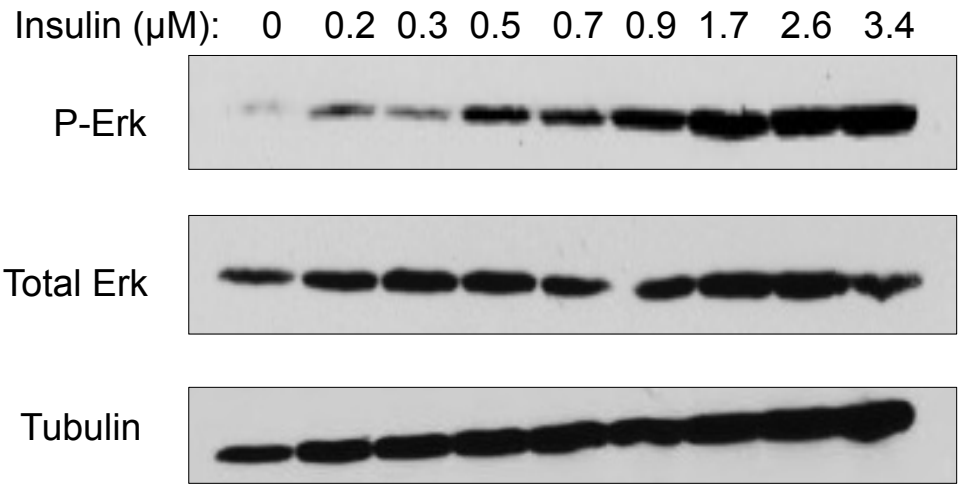

Figure S21

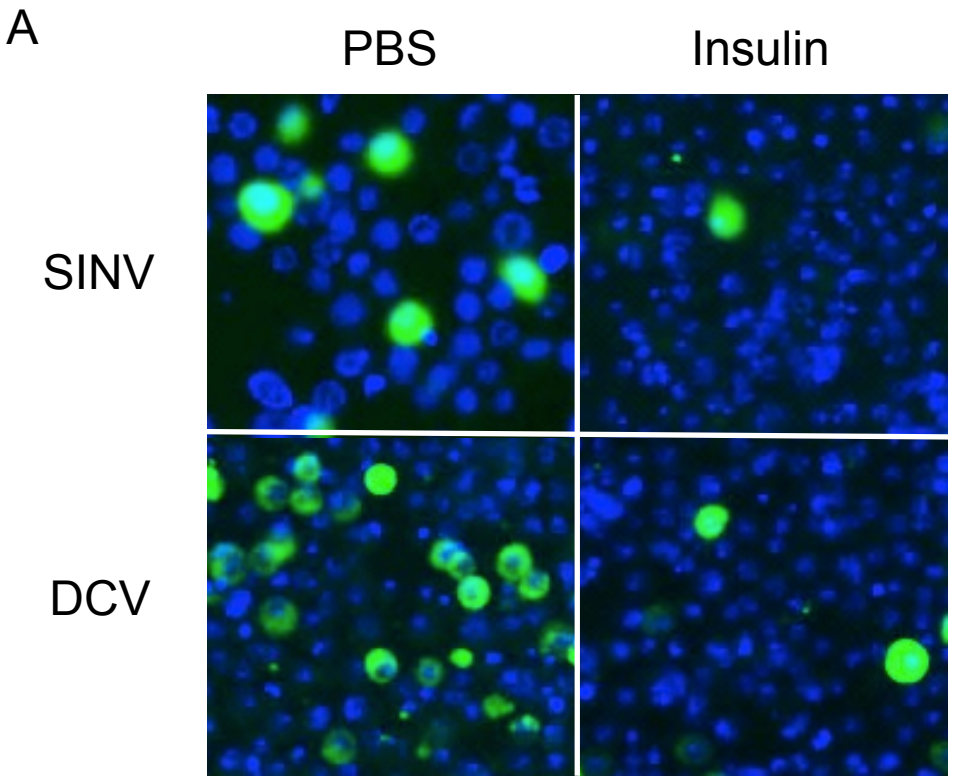
A
PBS
Insulin
SINV
DCV

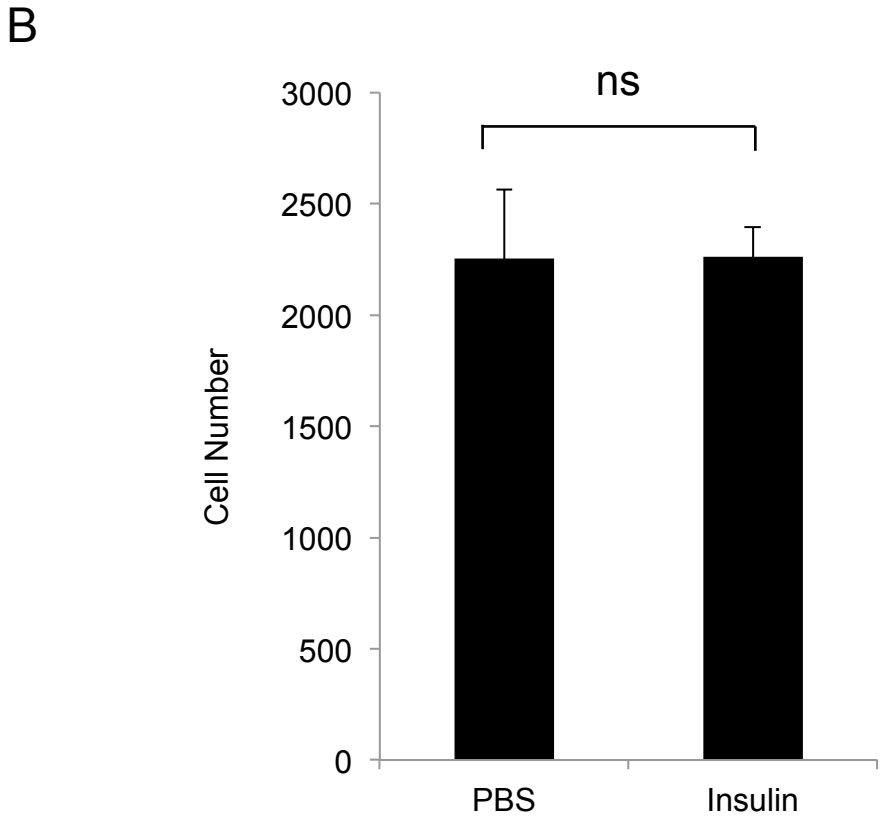
B
ns
3000
2500
2000
1500
1000
500
0
Cell Number
PBS
Insulin

Figure S22

A

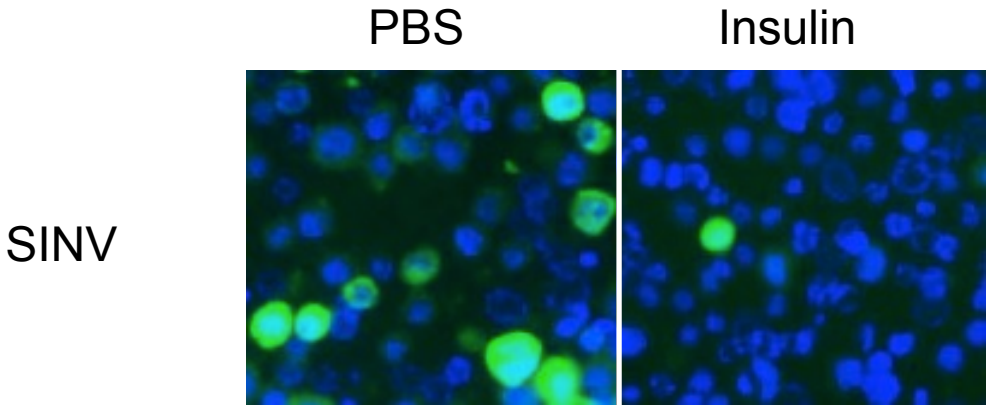

B

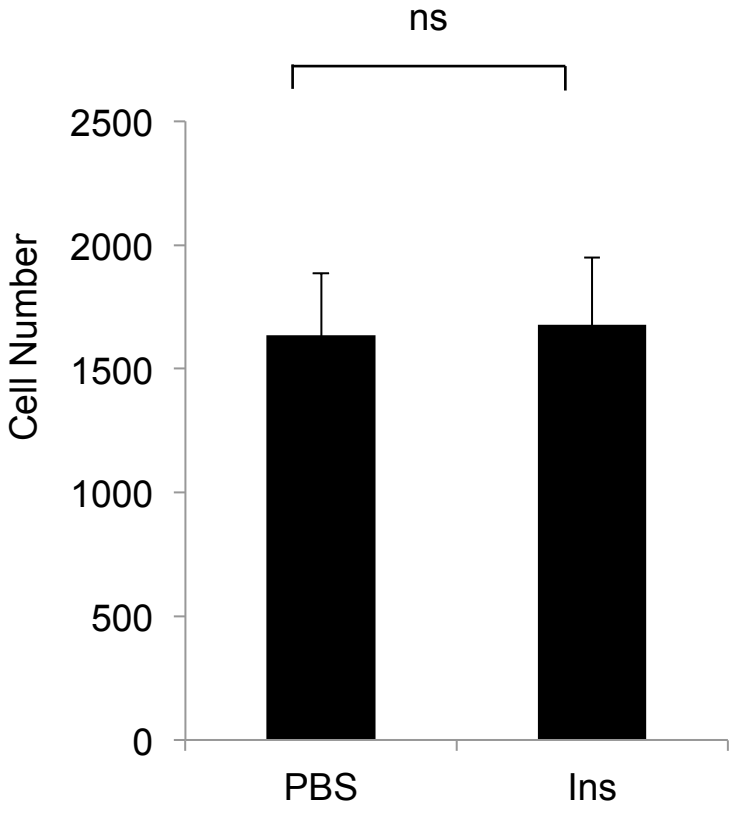

Figure S23

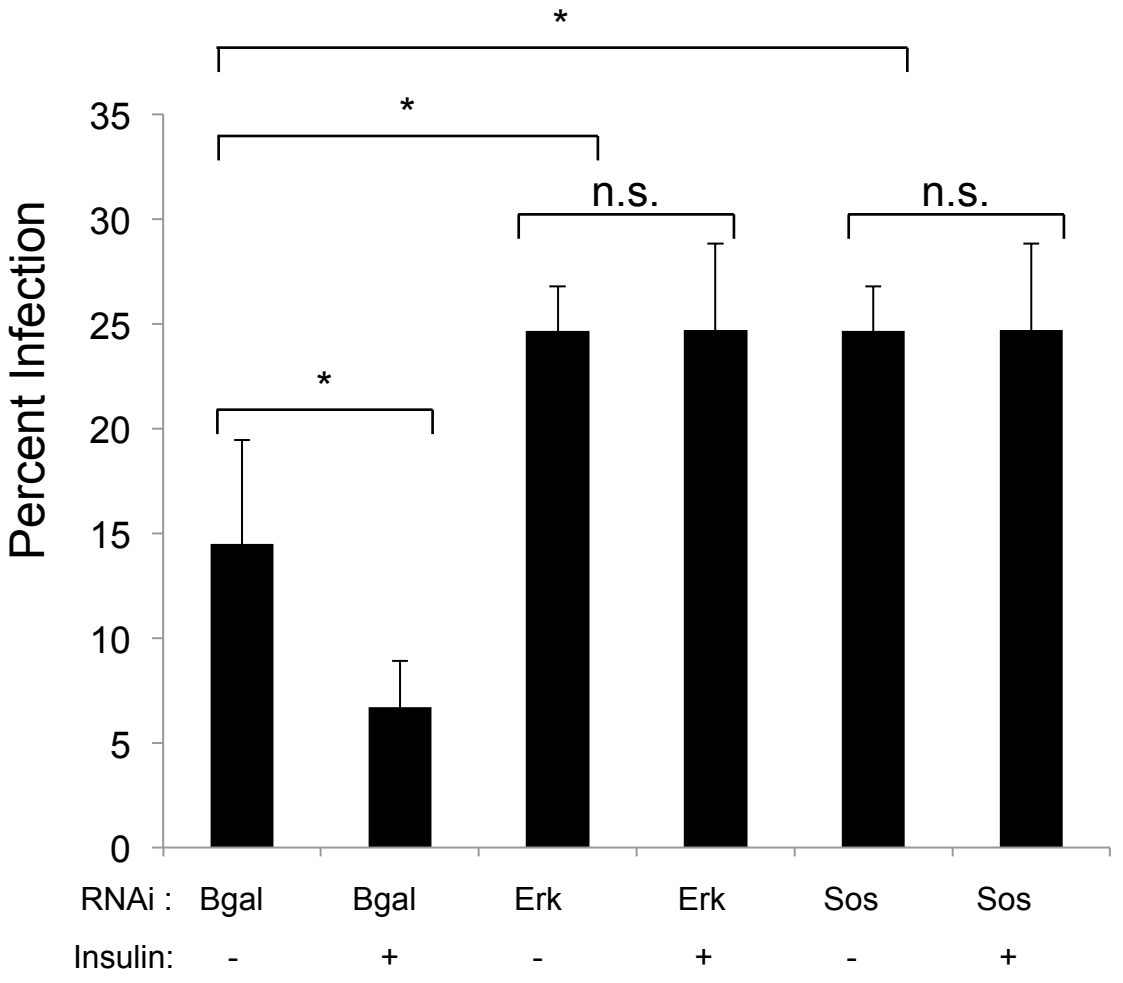
*
*
n.s.
n.s.
*
Percent Infection
35
30
25
20
15
10
5
0
RNAi :
Bgal
Bgal
Erk
Erk
Sos
Sos
Insulin:
-
+
-
+
-
+

Figure S24

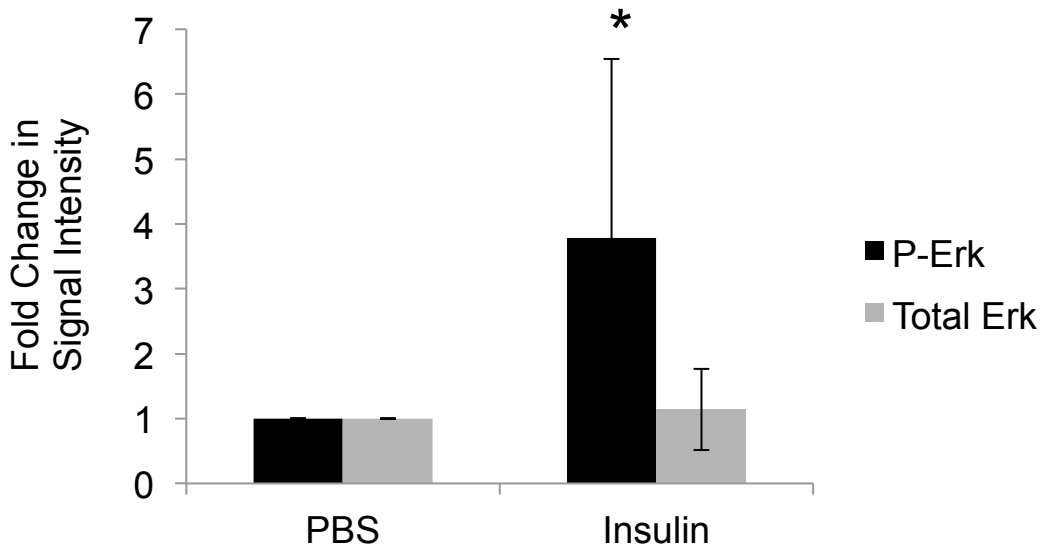
Fold Change in Signal Intensity
7
6
5
4
3
2
1
0
*
PBS
Insulin
P-Erk
Total Erk

Figure S25

A

B

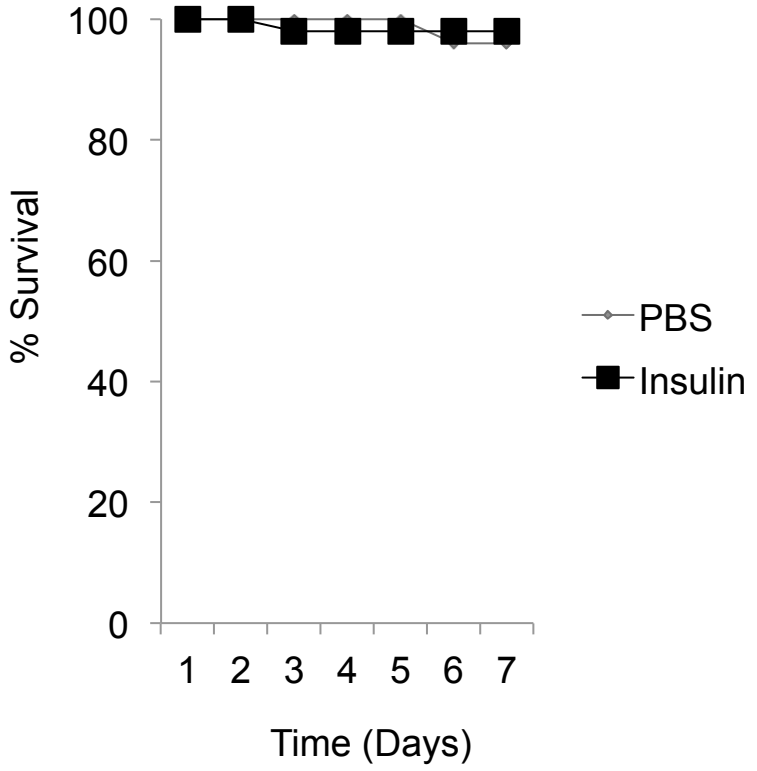

Figure S26

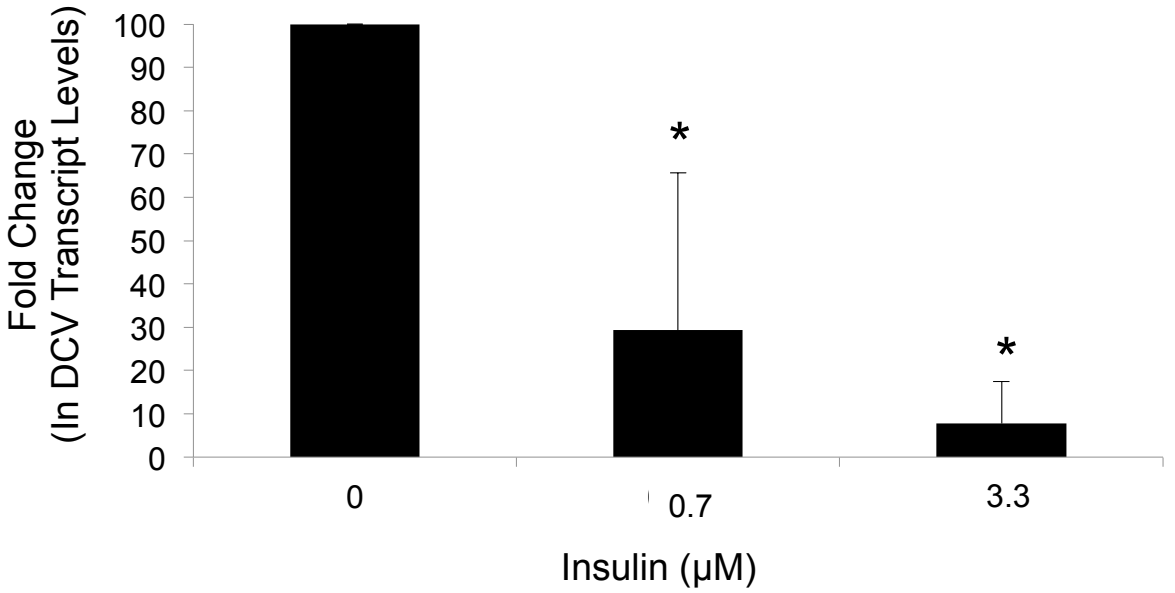
Fold Change
(In DCV Transcript Levels)
100
90
80
70
60
50
40
30
20
10
0
*
*
0
0.7
3.3
Insulin (μM)

Figure S27

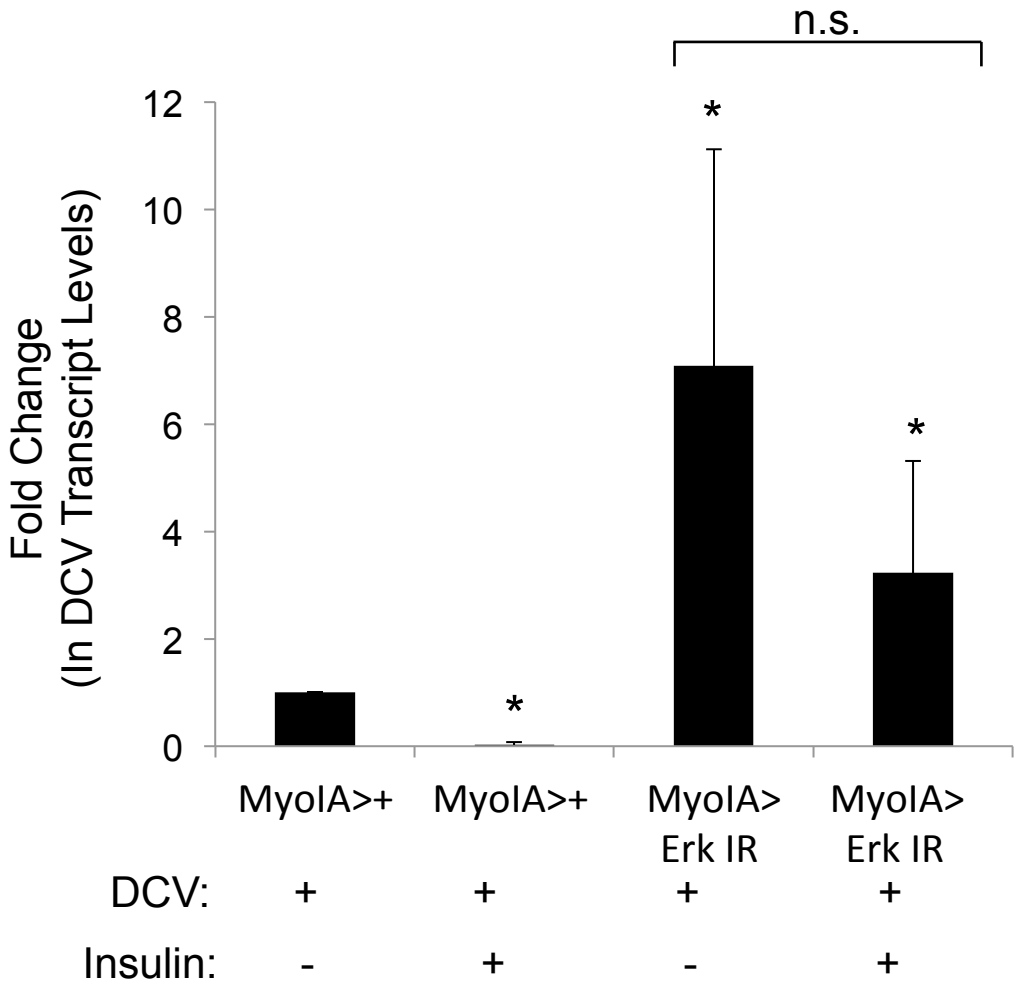
n.s.
*
*
*
12
10
8
6
4
2
0
Fold Change
(ln DCV Transcript Levels)
MyoIA>+
MyoIA>+
MyoIA>
Erk IR
MyoIA>
Erk IR
DCV:
+
+
+
+
Insulin:
-
+
-
+

Figure S28

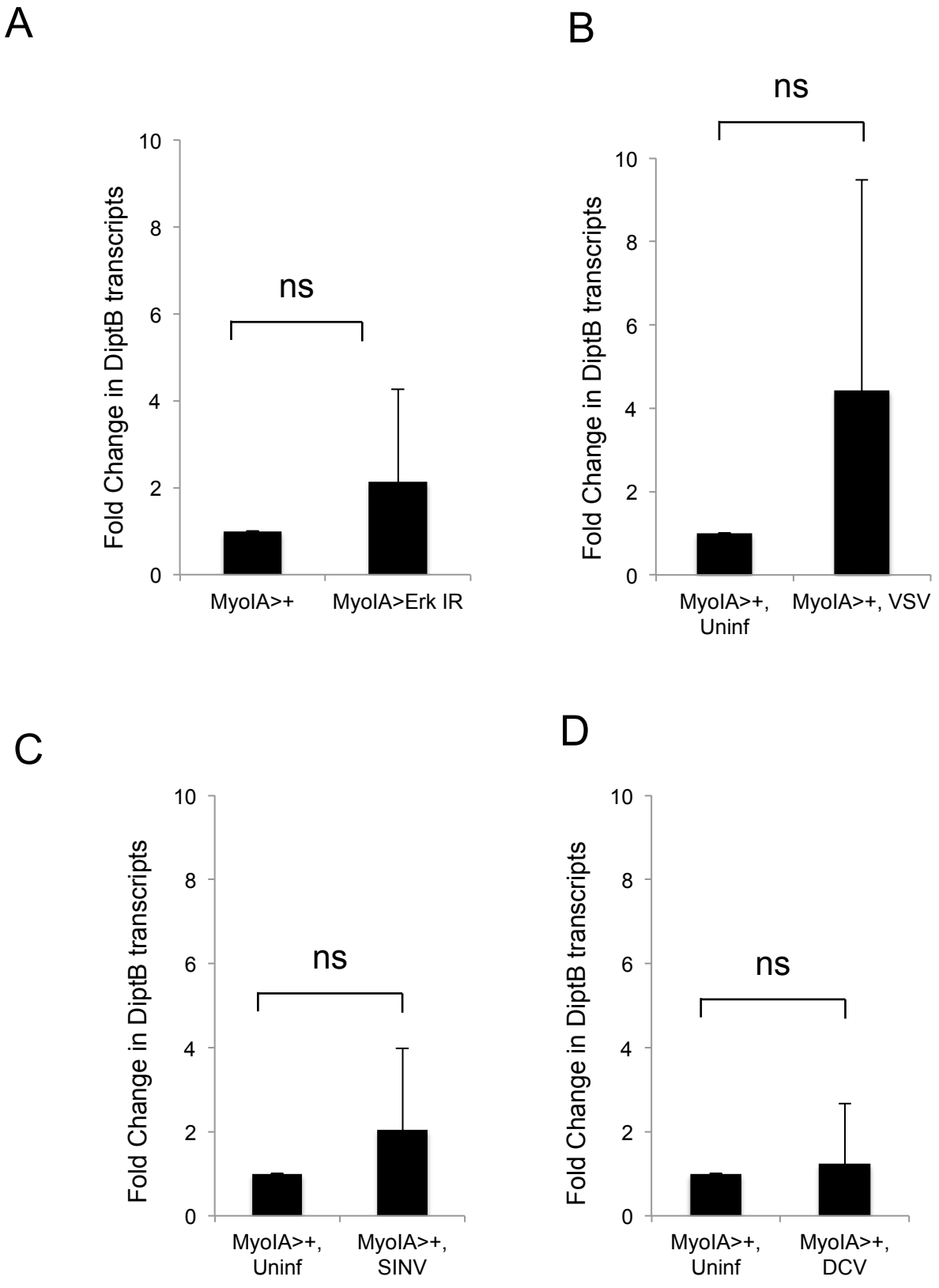
A
Fold Change in DiptB transcripts
10
8
6
4
2
0
ns
MyoIA>+
MyoIA>Erk IR
B
Fold Change in DiptB transcripts
ns
MyoIA>+, Uninf
MyoIA>+, VSV
C
Fold Change in DiptB transcripts
ns
MyoIA>+, Uninf
MyoIA>+, SINV
D
Fold Change in DiptB transcripts
ns
MyoIA>+, Uninf
MyoIA>+, DCV

Figure S29

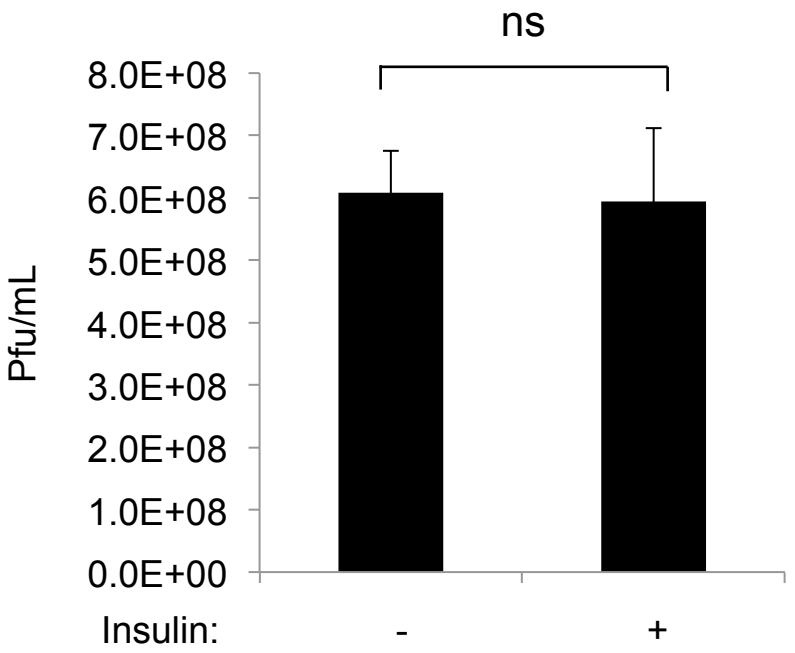
ns
8.0E+08
7.0E+08
6.0E+08
5.0E+08
4.0E+08
3.0E+08
2.0E+08
1.0E+08
0.0E+00
Pfu/mL
Insulin:
-
+

Figure S30